

**AES/PE/14-24**

**Comparative study of foam stability in bulk  
and porous media**

**15-9-2014**

**VJ van der Bent**

Title : Comparative study of Foam Stability in bulk and porous media

Author(s) : VJ van der Bent

Date : September 20014

Professor(s) : C.P.J.W. van Kruijsdijk

Supervisor(s) : S. Vincent-Bonnieu  
: S.A. Jones

TA Report number : AES/PE/14-24

Postal Address : Section for Petroleum Engineering  
Department of Geoscience & Engineering  
Delft University of Technology  
P.O. Box 5028  
The Netherlands

Telephone : (31) 15 2781328 (secretary)


Telefax : (31) 15 2781189

Copyright ©2014 Section for Petroleum Engineering

*All rights reserved.*

*No parts of this publication may be reproduced,  
Stored in a retrieval system, or transmitted,  
In any form or by any means, electronic,  
Mechanical, photocopying, recording, or otherwise,  
Without the prior written permission of the  
Section for Petroleum Engineering*

---



DELFT UNIVERSITY OF TECHNOLOGY

MASTER'S THESIS

---

# Comparative study of Foam Stability in bulk and porous media

---

*Author:*  
V.J. van der Bent

*Supervisors:*  
Prof. Ir. C.P.J.W. van Kruijsdijk  
Dr. S. Vincent-Bonnieu  
Dr. S.A. Jones





## *Abstract*

The oil recovery from a reservoir can be enhanced by gas injection. Creating a foam with the injected gas can improve the sweep efficiency. For an efficient foam displacement process the foam films must remain stable in the presence of oil. Unfortunately, most foams are destabilised by oil. It is therefore important to select a foaming agent appropriate for the reservoir. To select this foaming agent a reliable screening procedure is necessary.

In this thesis seven different surfactant solutions were screened using three experimental methods (Interfacial and surface tension measurements, bulk foam tests and core flooding experiments). The different experiments are performed both in the absence and presence of a paraffin oil, at a temperature of 50°C and atmospheric pressure.

The bulk foam experiments were carried out with the Foamscan apparatus. All the foams were destabilised by the oil, as predicted by the stability criteria about foam oil interaction. The rate of destabilisation is not accurately predicted and therefore the criteria have only limited applicability.

The core flood experiments were performed using a Lilliput core, which had a diameter of one centimetre. This Lilliput core flood set-up proved itself as a good surfactant screening tool. Bulk foam stability and the apparent viscosity in the core correlate well, in the absence of oil, this indicates that bulk foam experiments are a useful screening tool to predict the surfactant performance in a core flood experiment. In the presence of oil the behaviour in core floods was more complex and no good correlation was found with the bulk foam experiments.



# *Acknowledgements*

Special thanks should be given to my supervisors Prof. Ir. Cor van Kruijsdijk, Dr. Sebastien Vincent-Bonnieu and Dr. Siân Jones for their guidance, time and advises during this thesis.

I want to thank Prof. dr. Bill Rossen for sharing his knowledge, ideas and his valuable comments.

I also express my thankfulness to Dr. Rouhi Farajzadeh, Dr. Lori Pretzer and Dr. Leon Kapetas for their valuable input throughout this thesis.

I would also like to extend my thanks to all the members of both the Dietz lab and the Shell lab for their help and advices. In special Michiel Slob for his valuable technical support on the Lilliput core flood set-up and Menno van Haasterecht for providing the equipment and materials needed for this research.

This thesis has been written in collaboration with Shell Global Solutions International B.V. this gave me an unique combination of practical research and professional experiences. I very much appreciate the opportunity Shell gave me.

*Vincent van der Bent*  
*Katwijk, September 2014*





# Contents

<b>Abstract</b>	<b>iii</b>
<b>Acknowledgements</b>	<b>v</b>
<b>Contents</b>	<b>vi</b>
<b>List of Figures</b>	<b>xi</b>
<b>List of Tables</b>	<b>xiii</b>
<b>1 Introduction</b>	<b>1</b>
1.1 Foam used in enhanced oil recovery . . . . .	1
1.2 Objective of this thesis . . . . .	2
<b>2 Theory</b>	<b>3</b>
2.1 Foam . . . . .	3
2.2 Surfactants . . . . .	3
2.2.1 Surfactants and film stability . . . . .	4
2.2.2 Surfactants and surface tension . . . . .	4
2.2.3 Surface elasticity . . . . .	4
2.3 Conditions for local stability in foam . . . . .	5
2.3.1 Laplace capillary pressure . . . . .	5
2.3.2 Disjoining pressure . . . . .	6
2.4 Foam stability . . . . .	8
2.4.1 Gravity drainage . . . . .	8
2.4.2 Coarsening and coalescence . . . . .	8
2.5 Foam stability in the presence of oil . . . . .	9
2.5.1 Spreading, entering and bridging coefficient . . . . .	10
2.5.2 Lamella number . . . . .	12
2.5.3 Pseudo-emulsion film . . . . .	13
2.5.4 Summarised results of previous studies . . . . .	13
2.6 Foam in porous media . . . . .	15
2.6.1 Mobility reduction . . . . .	15
2.6.2 Foam generation in porous media . . . . .	15
Snap-off . . . . .	15
Lamella division . . . . .	15
Leave behind . . . . .	16

2.6.3	Foam destruction in porous media . . . . .	17
<b>3</b>	<b>Bulk foam stability</b>	<b>19</b>
3.1	Introduction . . . . .	19
3.2	Experimental description . . . . .	19
3.2.1	Materials . . . . .	19
3.2.2	Solution stability . . . . .	20
3.2.3	Measurement of interfacial properties . . . . .	21
3.2.4	Bulk foam experimental set-up . . . . .	21
3.2.5	Experimental procedure . . . . .	22
3.2.6	Bubble size measurement . . . . .	22
3.3	Results . . . . .	23
3.3.1	Interfacial properties . . . . .	23
3.3.2	Foamability . . . . .	24
3.3.3	Bubble size . . . . .	24
3.3.4	Bulk foam stability . . . . .	25
3.3.5	Stability criteria . . . . .	28
3.4	Discussion . . . . .	28
3.4.1	Foamability . . . . .	28
3.4.2	Surface tension . . . . .	29
3.4.3	Entering, spreading and bridging coefficient . . . . .	29
3.4.4	Lamella number . . . . .	30
3.4.5	Interfacial tension . . . . .	30
3.5	Conclusions . . . . .	31
<b>4</b>	<b>Foam in porous media</b>	<b>33</b>
4.1	Introduction . . . . .	33
4.2	Core flooding theory . . . . .	33
4.3	Experimental description . . . . .	35
4.3.1	Materials . . . . .	35
4.3.2	Core and core holder . . . . .	36
4.3.3	Experimental set-up . . . . .	36
4.3.4	Experimental procedure . . . . .	37
4.3.4.1	Initial core set up . . . . .	37
4.3.4.2	Core flood procedure . . . . .	38
4.4	Results . . . . .	38
4.5	Discussion . . . . .	40
4.5.1	Set-up . . . . .	40
4.5.2	Experimental results . . . . .	41
4.5.3	Rheology in the low quality regime . . . . .	42
4.6	Conclusions . . . . .	43
<b>5</b>	<b>Foam in porous media in the presence of oil</b>	<b>45</b>
5.1	Introduction . . . . .	45
5.2	Experimental description . . . . .	45
5.2.1	Materials and experimental set-up . . . . .	45
5.2.2	Experimental procedure . . . . .	45

---

5.3	Results . . . . .	46
5.4	Discussion . . . . .	49
5.4.1	Oil saturation . . . . .	49
5.4.2	Discussion of experimental results . . . . .	49
5.4.3	Residual oil saturation during the experiment . . . . .	52
5.4.4	Stability criteria . . . . .	52
5.5	Conclusions . . . . .	53
<b>6</b>	<b>Relation between bulk foam and porous media foam</b>	<b>55</b>
6.1	Bulk foam and foam in porous media . . . . .	55
6.2	Bulk foam and foam in porous media in the presence of oil . . . . .	57
6.3	Conclusions . . . . .	57
<b>7</b>	<b>Curve fitting</b>	<b>59</b>
7.1	Introduction . . . . .	59
7.2	STARS model . . . . .	59
7.3	Results and discussion . . . . .	60
7.4	Conclusions . . . . .	61
<b>8</b>	<b>Conclusion and future directions</b>	<b>63</b>
8.1	Conclusion . . . . .	63
8.2	Future directions . . . . .	65
8.3	Recommendations to improve experiment results . . . . .	65
8.3.1	Recommendations for bulk foam experiments . . . . .	65
8.3.2	Recommendations for the core flood experiments in the absence of oil . . . . .	66
8.3.3	Recommendations for the core flood experiments in the presence of oil . . . . .	66
<b>A</b>	<b>Results core flood experiments</b>	<b>67</b>
<b>B</b>	<b>Interfacial rheology measurement</b>	<b>71</b>
B.1	Surface rheology . . . . .	72
B.2	Materials . . . . .	72
B.3	Results . . . . .	73
<b>C</b>	<b>Results curve fitting</b>	<b>75</b>
	<b>Bibliography</b>	<b>77</b>



# List of Figures

2.1	A thin film stabilised by surfactant molecules. . . . .	4
2.2	Surface tension as a function of the surfactant concentration, adapted from Schramm <sup>1</sup> . . . . .	5
2.3	A sketch demonstrating the Gibbs-Marangoni effect. The locally lowered surfactant concentration causes contraction of the surface. . . . .	5
2.4	Illustration of a foam film between two Plateau borders. . . . .	6
2.5	Schematic disjoining pressure isotherm, adapted from <sup>2</sup> . . . . .	7
2.6	Foam in equilibrium, after drainage. The bubbles at the foam-liquid interface are spherical while the top of the foam is dryer and the bubbles are polyhedral. . . . .	9
2.7	The forces acting on an oil droplet. . . . .	10
2.8	A schematic representation of the meaning of the entry coefficient. . . . .	10
2.9	A schematic representation of the meaning of the bridging coefficient. . . . .	11
2.10	The three different foam generation mechanisms in porous media. . . . .	16
3.1	Schematic overview of the Foamscan device adapted from manufacturer TECLIS. . . . .	22
3.2	Schematic overview of the set-up, used to determine the bubble size. . . . .	23
3.3	Samples of wet foam generated in the Foamscan for each surfactant solution. The foams are polydisperse, but the range of bubble sizes is fairly consistent for all the samples studied. . . . .	26
3.4	The average (n=2) half-life of the seven different solutions in the absence and the presence of oil. . . . .	27
3.5	The foam volume plotted over time for three bulk foam experiments with solution 3 in the presence of oil. . . . .	27
3.6	The half-life of the foam in the absence of oil is plotted against all the associated surface tension for all the solutions tested. . . . .	29
3.7	A plot of the foam half-life as a function of the interfacial tensions of the surfactant solution with Isopar H. . . . .	31
4.1	A schematic representation of the pressure gradient contours as a function of the liquid and gas velocity . . . . .	34
4.2	An example of a curve obtained with a fixed total flow rate . . . . .	35
4.3	Schematic diagram of the Lilliput core flood set-up. . . . .	37
4.4	The pressure drop over the core versus the number of pore volumes injected. (This curve was obtained with solution 7 at $f_g = 0.30$ ) . . . . .	39
4.5	Foam quality scan curves, obtained with four different surfactant solutions. . . . .	40
4.6	The maximum apparent viscosity plotted as a function of $f_g^*$ (from the data in table 4.2). . . . .	42

---

5.1	Foam quality scan curves for all the solutions in the presence of oil. . . . .	47
5.2	The performance of the different surfactant solution in porous media in the presence of oil and in an oil free porous media. . . . .	48
5.3	The capillary number at different foam qualities. . . . .	50
5.4	This graph shows the amount of time needed to reach a steady pressure drop with and without oil. The data was obtained with solution 7 at a foam quality of 0.5 . . . . .	51
5.5	The measured pressure drop over time is shown. The first measurement with oil is done at the beginning of the experiment and the second measurement at the end of the experiment. The tests are performed with solution 5 at a foam quality of 0.05 . . . . .	52
6.1	The half-life and maximal apparent viscosity of the used surfactant solutions plotted in one graph. . . . .	56
6.2	The half-life and the maximal apparent viscosity of the surfactant solution in the presence of oil. . . . .	58
7.1	An example of the modelled curve and the experimental data. . . . .	62
A.1	The pressure drop over the core for all the surfactants solution measured in the absence of oil. . . . .	68
A.2	The apparent viscosity of all the surfactant solutions at different foam qualities in the absence of oil. . . . .	69
A.3	The pressure drop over the core for all surfactant solutions measured in the presence of oil. . . . .	70
B.1	Overview of the double wall ring rheometer. The torque is increased due to the double wall geometry of the ring used <sup>3</sup> . . . . .	72
B.2	The loss modulus as function of angular frequency for the used solutions. . . . .	73
C.1	The experimental data for the six different surfactant solutions in the absence of oil and their associated model curves. . . . .	76

# List of Tables

2.1	The work of different authors summarised. If the results of the author agree with the stability criteria the box is marked green, otherwise the box is red. . . . .	14
3.1	The type of surfactants used in the different solutions. (*Dodecanol is a fatty alcohol). . . . .	20
3.2	Properties of the used paraffin oil, Isopar H. . . . .	20
3.3	Interfacial properties of the surfactant solutions at 20°C and 55°C (SFT is the surface tension with air and IFT is the interfacial tension with Isopar H. . . . .	24
3.4	Average time (n=2) needed to get 100 ml foam, with and without oil. . .	24
3.5	The mean bubble radius, the standard deviation and $\beta$ of the different solutions tested. . . . .	25
3.6	The different coefficients and the lamella number for all the surfactants. Green indicates the best, and red the worst (predicted) performance *Half-life in the presence of oil. . . . .	28
4.1	Properties of the used Bentheimer sandstone core used for the liliput core flood tests. . . . .	36
4.2	Summary of the highest pressure gradient and apparent viscosity measured, $f_g^*$ indicates the foam qualities at which these maxima occurred. . . . .	40
5.1	The performance of all the surfactant solutions, both in the presence and absence of oil. . . . .	47
5.2	The different coefficients and the lamella number listed in one table. Green indicates the best and red the worst performance (actual or predicted) $\mu_{app}$ in the presence of oil. . . . .	53
6.1	The viscosities of the bulk liquid, measured at 55.0 °C . . . . .	57
7.1	Overview of values of the five parameters from the STARS model used to fit the data. . . . .	61





# Chapter 1

## Introduction

### 1.1 Foam used in enhanced oil recovery

Gas flooding is one of the most generally accepted and widely used methods to enhance the oil production<sup>4</sup>. The basic mechanism responsible for the increased recovery with a gas flood is the improved microscopic sweep efficiency<sup>5</sup>. The injected gas partly dissolves into the oil and causes the oil to swell. This results in the mobilisation of residual oil trapped in inaccessible pore spaces. The swelling also reduces the viscosity of the oil and lowers the interfacial tension between the oil and the displacing phase. However, a drawback with gas flooding is the poor volumetric sweep caused by two separate issues. Firstly, the big difference in viscosity between the gas and the crude oil results in an unfavourable mobility ratio. This results in an unstable displacement, unwanted fingering will occur and the gas will eventually create pathways to the production well. Reservoir heterogeneities can amplify this effect. Secondly, the displacing gas tends to move upwards in the reservoir, due to the low density compared to the fluids, and gravity override can occur<sup>6</sup>. These two effects cause a poor volumetric sweep, this means that the gas will only interact with a small fraction of the oil and therefore the total recovery will be low after a gas flood.

A possible solution to the gas flooding problems is to foam the injected gas. The apparent viscosity of the foam is much higher than the gas viscosity, therefore the mobility of the gas is drastically reduced. This results in a more stable displacement process. Foam has lower mobility in higher permeable layers and will therefore reduce or block the flow in these layers. The flow will be diverted to the unswept parts of the reservoir.

A major concern with the application of foam as an enhanced oil recovery (EOR) method is the stability of foam when it comes into contact with the crude oil. The foam must

remain stable in the reservoir for a successful foam-flood<sup>7,8</sup>. To effectively generate such a foam, appropriate foaming agents should be selected<sup>7,9,10</sup>.

## 1.2 Objective of this thesis

It is important to select the appropriate foaming agent in order to successfully use foam for enhanced oil recovery. The foaming agent is field and application specific and a screening is required to pick the right foaming agent. The different techniques used to screen the surfactants are analysed in this study. The objectives of this thesis are:

- Investigate the different theories about the stability of foam in the presence of oil and investigate if these theories are applicable for foam in porous media.
- Investigate the usefulness of bulk foam tests in a surfactant screening for foam EOR by investigating if there is a correlation between the stability of bulk foam and foam in porous media.
- Investigate the effect of surfactant type on the STARS foam model, to evaluate which parameters are influenced by surfactant type.

## Chapter 2

# Theory

### 2.1 Foam

When bubbles congregate together to form a foam, they create structures that change and evolve as they age<sup>11</sup>. Foams may be relatively wet or dry, dependent on the amount of liquid they contain. A foam is considered "dry" when the liquid fraction is below 1% and "wet" for liquid fraction between 1% and 30%. For liquid fractions above 30% the foam is considered as a bubbly liquid<sup>12</sup>. A foam always aims to minimise the surface area of the liquid films that separate the gas bubbles. Therefore the structure of foam changes from a close-packing of spheres in its wet limit to a polyhedral cell structure in the dry limit. Dry foam obeys the rules formulated by Joseph Plateau, from his experimental observations<sup>13</sup>:

- Three (and only three) films meet, at  $120^\circ$  in a Plateau border.
- In a 3D foam Plateau borders always meet symmetrically in fours, at an angle of  $109.47^\circ$ .

### 2.2 Surfactants

Generally, surfactants are needed to create foam. Surfactants are chemical compounds that have great influence on the surface and interface properties. The molecules are composed of two parts; one part that has affinity for polar media and another part that has affinity for non-polar media. Therefore the molecules tend to form layers at interfaces. Surfactant molecules are responsible for two important effects; stabilising foam films and reducing the interfacial tension.

### 2.2.1 Surfactants and film stability

A bubble can only be stable when the interface is stabilised by surfactant molecules. A thin film, also called a lamella, consists of two monolayers of surfactant molecules, with the liquid phase in between (figure 2.1). There is a repulsive force between the surfactant mono-layers, causing a static stability.

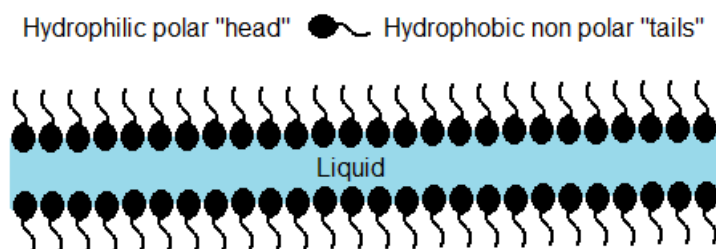


FIGURE 2.1: A thin film stabilised by surfactant molecules.

### 2.2.2 Surfactants and surface tension

In the bulk water the molecules form strong cohesive bonds with surrounding molecules. At the water surface however the molecules have fewer neighbours to bonds, therefore these molecules exhibit stronger attractive forces upon their nearest neighbours. The increased attractive force at the surface is called surface tension. Surfactant molecules bond to the water molecules at the interface, and prevent water molecules from binding as tightly to one another, hence lowering the surface tension.

Surfactants will not only form layers at the interfaces. When the concentration becomes higher, surfactant molecules will also interact with each other and form micelles, i.e. surfactant molecules packed together within the bulk of the fluid. The surfactant concentration at which the molecules start to interact with one another is called the critical micelle concentration (cmc). Higher surfactant concentrations will not reduce the surface tension any further (figure 2.2). The cmc depends on the surfactant used, but also has a weak dependence on pressure and temperature.

### 2.2.3 Surface elasticity

Foam films should have some elasticity in order to be able to withstand small deformations without rupturing. The Gibbs-Marangoni effect<sup>14</sup> is responsible for this elasticity. When a surfactant stabilised liquid film undergoes an expansion the surfactant concentration is lowered locally (figure 2.3). The lower surfactant concentration results in a

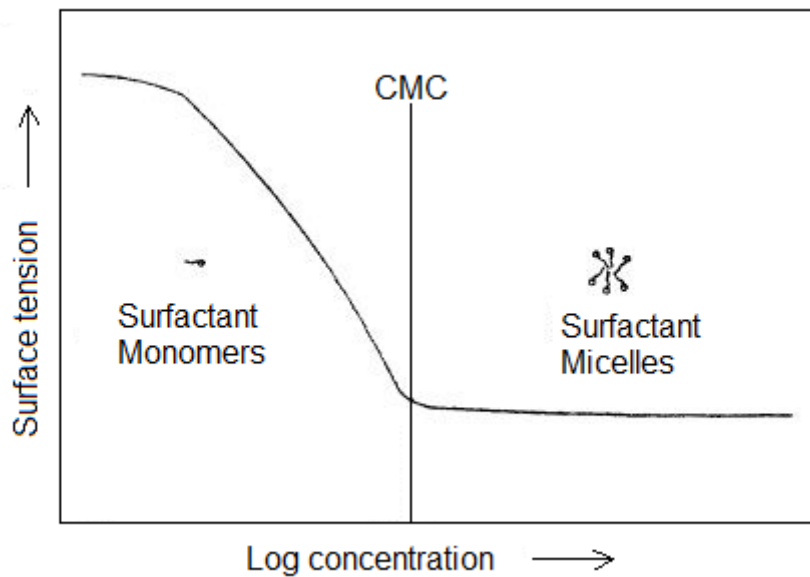


FIGURE 2.2: Surface tension as a function of the surfactant concentration, adapted from Schramm<sup>1</sup>.

locally higher surface tension, which causes a contraction of the expanded surface to maintain a low energy. This effect provides resistance against film thinning, which could eventually lead to film rupture.

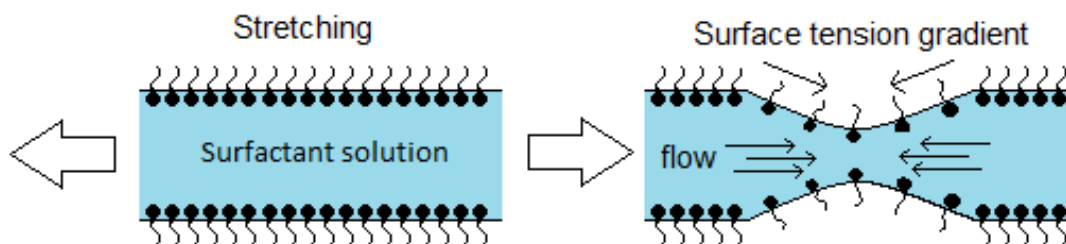


FIGURE 2.3: A sketch demonstrating the Gibbs-Marangoni effect. The locally lowered surfactant concentration causes contraction of the surface.

## 2.3 Conditions for local stability in foam

### 2.3.1 Laplace capillary pressure

Laplace capillary pressure causes a liquid flow from the films to the Plateau borders, due to the difference in the curvature of the liquid surface. Figure 2.4 shows the difference in

curvature for a liquid film in between two Plateau borders. The Young–Laplace equation describes how the pressure difference between the gas and liquid phase varies with the radius,  $R$  of the curved interface.

$$\Delta P = P_G - P_L = \frac{2\gamma}{R} \quad (2.1)$$

where  $P_G$  is the gas pressure,  $P_L$  the liquid pressure and  $\gamma$  the surface tension. The quantity  $P_G - P_L$  is also known as the capillary pressure  $P_c$ . The radius of curvature at the surface of the Plateau border,  $R_2$  is smaller than the radius of curvature of the thin liquid film,  $R_1$ . The gas pressure  $P_G$  in the bubble is equal, therefore there must be a pressure difference within the liquid phase. The liquid in the Plateau border has a lower pressure than the liquid in the film. Due to this pressure difference liquid flows from the films to the Plateau borders.

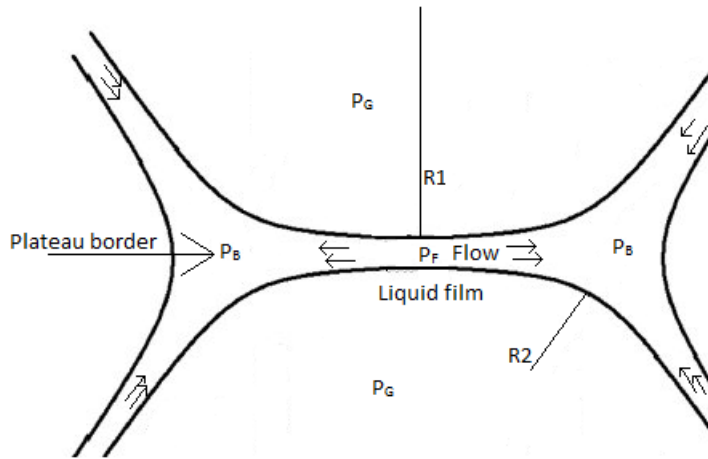


FIGURE 2.4: Illustration of a foam film between two Plateau borders.

### 2.3.2 Disjoining pressure

The pressure difference within the liquid phase causes film thinning. This is only stopped when the surfactant molecules at the outer surfaces of the lamella begin to interact with each other. The interaction between the surfaces of the lamella is called the disjoining pressure. There are three different components that contribute to the disjoining pressure,  $\Pi(h)$ : van der Waals forces,  $\Pi_{VW}$ , electrostatic forces,  $\Pi_{EL}$  and steric forces,  $\Pi_S$ .

$$\Pi_T(h) = \Pi_{EL} + \Pi_{VW} + \Pi_S \quad (2.2)$$

The attractive van der Waals forces have a negative contribution to the disjoining pressure. The electrostatic forces stabilise the foam film. When equally charged interfaces

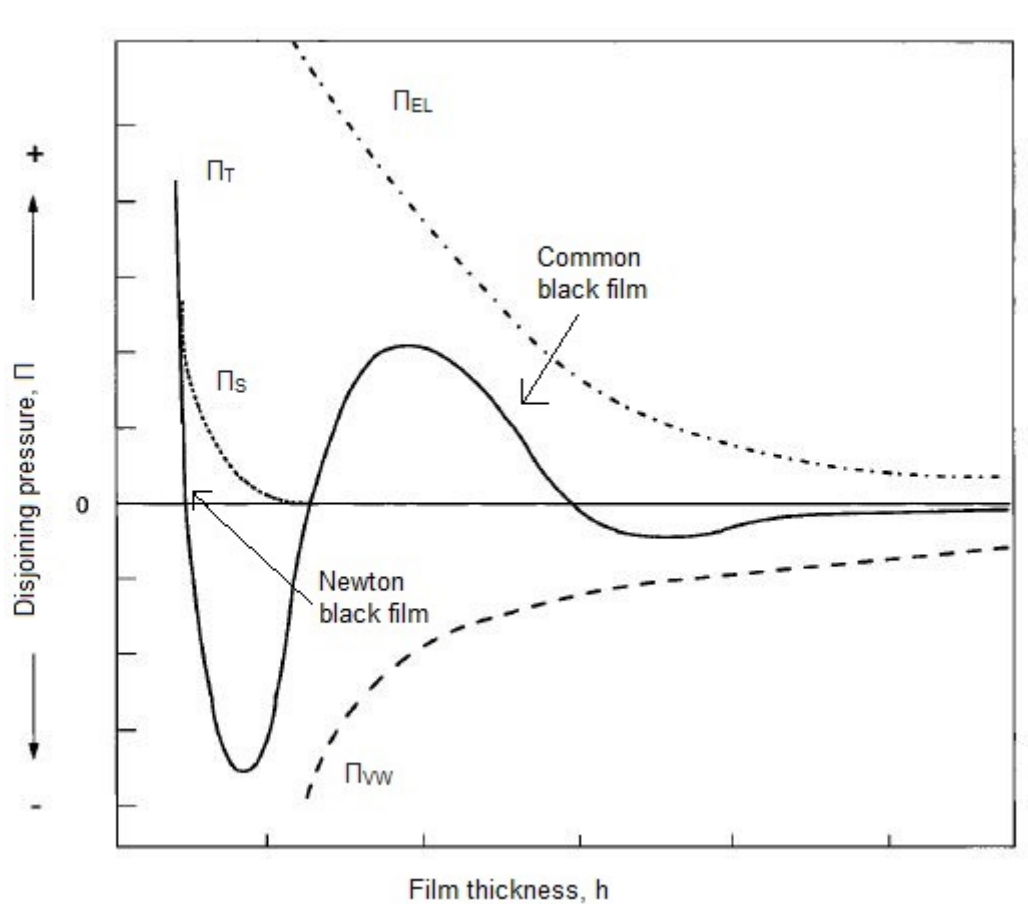


FIGURE 2.5: Schematic disjoining pressure isotherm, adapted from<sup>2</sup>.

approach each other and their electric double layers overlap, a repulsive force will be created, which is a positive contribution to  $\Pi_T$ . The steric forces arise from the fact that each atom within a molecule occupies a certain amount of space, they are repulsive and only observed at very short length scale. Molecule size can be important for steric interaction<sup>15</sup>.

The magnitude and the sign of the total disjoining pressure vary with the film thickness  $h$  (figure 2.5). When the film thickness is decreasing, a local maximum in disjoining pressure is encountered. The repulsive overlap of the electrostatic double layer is overpowering the van der Waals attraction. Films on this branch are called common black films. If the film thickness decreases further, van der Waals forces become more dominant. Stability is reached again when steric forces become significant, these films are called Newton black films.

When the system is in equilibrium the sum of the disjoining pressure and the pressure of the liquid phase is equal to the gas pressure. As seen in equation (2.3) the capillary pressure is counterbalanced by the disjoining pressure<sup>2</sup>.

$$\begin{aligned}\Pi(h) + P_L &= P_G, \\ \Pi(h) &= P_G - P_L = P_C\end{aligned}\tag{2.3}$$

## 2.4 Foam stability

Foams are not thermodynamically stable: once the generation of the foam is stopped, foam volume will decay. The liquid will drain out of the foam and the average bubble size will increase with time<sup>12</sup>.

### 2.4.1 Gravity drainage

Gravity is responsible for the separation of the gas and the liquid. With time the liquid drains out of the foam, drainage creates a gradient in the liquid fraction (figure 2.6). The foam structure changes from spherical bubbles in a wet foam to polyhedral shaped bubbles in a dry foam. The Plateau border radius in the wet part of the foam is bigger than in a dryer part<sup>16</sup>. Due to the Laplace–Young law, the capillary pressure in the liquid in the wet part must be higher than in the dry part. The resultant capillary forces work in opposite direction of the gravity forces and therefore reduce the drainage speed. The velocity of the fluid in the drainage process is slowed down by viscous processes that occur in the Plateau borders or in the nodes of the foams. A higher viscosity of the bulk fluid will therefore retard liquid drainage. Bubble size is also important, in foam with small bubbles the viscous dissipation is larger, drainage will therefore be slower.

### 2.4.2 Coarsening and coalescence

The average bubble size tends to increase with time as two bubbles merge and form one single bubble. There are two mechanisms responsible for the change in bubble size, coarsening and coalescence. Coarsening happens because gas can diffuse from one gas bubble to another. In a polydisperse foam, the gas bubbles have different sizes and the Laplace formula states that the bubble radius is inversely related to the gas pressure. Therefore small bubbles have a high gas pressure compared to large bubbles. This pressure difference causes gas to diffuse through the liquid from small bubbles to larger bubbles. The second mechanism, coalescence, causes an increase in the average bubble size due to the rupture of a lamella separating two bubbles. Coalescence always occurs at the top of the foam because it is liquid fraction (drainage) related. In the case of



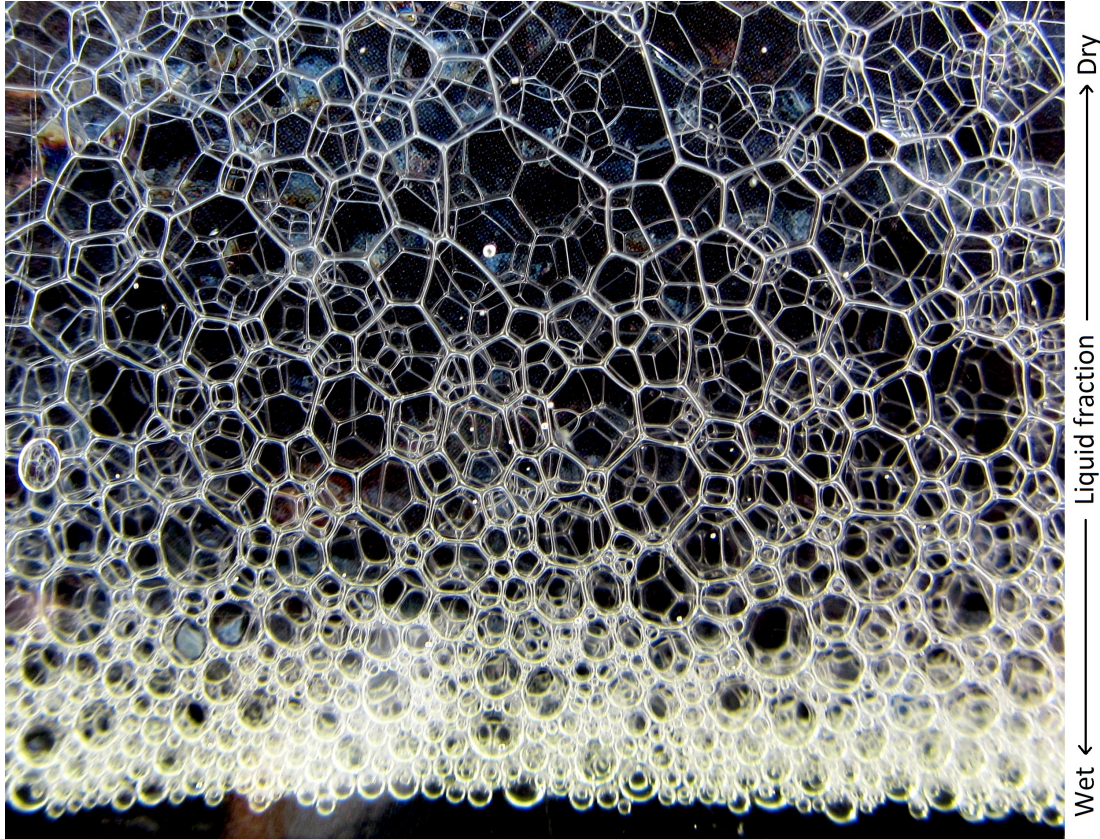


FIGURE 2.6: Foam in equilibrium, after drainage. The bubbles at the foam-liquid interface are spherical while the top of the foam is dryer and the bubbles are polyhedral.

large bubbles, coalescence events evolve in large avalanches, whereas the decrease of the height of fine foams is nearly continuous<sup>17</sup>.

## 2.5 Foam stability in the presence of oil

Foam is an attractive driving fluid for enhanced oil recovery, and can also be used to block the gas flow in certain parts of a reservoir. Unfortunately, (crude) oil destabilises most foams. In order to select the right foam for enhanced oil recovery it would be useful to be able to predict how the foam would interact with oil in the porous media, ideally from screening measurements on the bulk foam or bulk fluid only. Currently there are three main theories explaining foam oil interactions:

- Spreading, entering and bridging coefficients
- Lamella number
- Pseudo-emulsion film theory

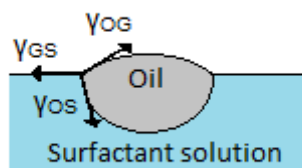


FIGURE 2.7: The forces acting on an oil droplet.

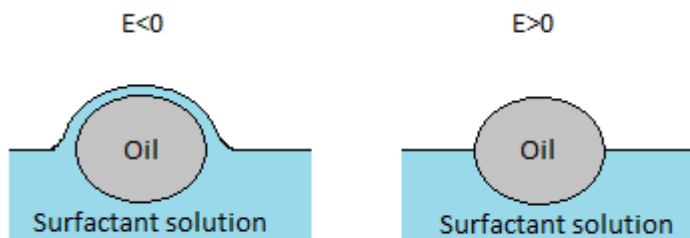


FIGURE 2.8: A schematic representation of the meaning of the entry coefficient.

### 2.5.1 Spreading, entering and bridging coefficient

Hydrophobic particles, in this case oil droplets, are able to destroy foam films. The ability of an oil droplet to disrupt the foam film is linked to three different interfacial tensions (figure 2.7). Firstly the surface tension between the aqueous solution and the gas phase,  $\gamma_{GS}$ , secondly the interfacial tension between the aqueous solution and the oil phase,  $\gamma_{OS}$ , and thirdly the interfacial tension between the oil phase and the gas phase  $\gamma_{OG}$ . There are three terms, based on these interfacial tensions that are used to give a prediction of foam stability in the presence of oil: the entering coefficient, E, the bridging coefficient, B and the spreading coefficient, S.

The entry coefficient is used to determine if it is thermodynamically favourable for the oil droplet to enter the solution gas surface.

$$E = \gamma_{GS} + \gamma_{OS} - \gamma_{OG} \quad (2.4)$$

If E is negative the oil droplet cannot enter the foam interface, and the surfactant solution completely wets the oil drop (figure 2.8).

When an oil drop fully breaks through the thin liquid film an oil bridge is formed (figure 2.9). The mechanical stability of a formed bridge can be determined with the bridging

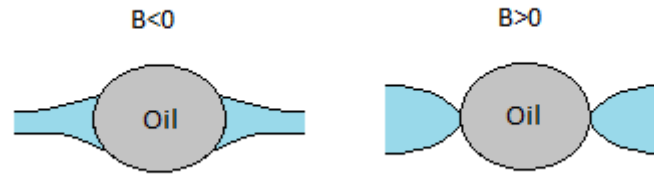


FIGURE 2.9: A schematic representation of the meaning of the bridging coefficient.

coefficient. If  $B$  is negative a stable bridge can be formed, if  $B$  is positive the bridge is unstable.

$$B = \gamma_{GS}^2 + \gamma_{OS}^2 - \gamma_{OG}^2 \quad (2.5)$$

Spreading oils have a negative effect on the foam stability. The spreading coefficient shows the ability of the oil to spread over the liquid gas interface.

$$S = \gamma_{GS} - \gamma_{OS} - \gamma_{OG} \quad (2.6)$$

A positive value of the spreading coefficient indicates an oil that will spread along the gas solution interface. A high spreading rate will have a negative effect on the foam stability. A negative spreading coefficient indicates that the oil will not spread.

The entering, spreading and bridging coefficients, described by Denkov et al.<sup>18</sup>, have been investigated by several people, but the conclusions as to whether these coefficients can predict foam stability are ambiguous (table 2.1). The stability of foam in porous media is related the spreading of the oil according to<sup>19,20,21</sup>. However, Lee et al.<sup>22</sup>, conclude that spreading alone is not sufficient to explain their observations in bulk foam and Manlowe and Radke<sup>23</sup> were unable to correlate the spreading coefficient and foam stability using a micro model. Mannhardt et al.<sup>24</sup> also found that there is no one-to-one correlation between the spreading or entering coefficient and foam stability in porous media. An entering coefficient below zero usually indicates a stable foam, and Dalland et al.<sup>21</sup> did observe this behaviour in porous media. Andrianov et al.<sup>25</sup> found that only very small values of the entering coefficient could be considered as a good indication of stable foam. According to Bergeron et al.<sup>26</sup> the classic form of the entering coefficient gives at best an indication of foam stability in porous media, because it neglects much of the relevant physics of the porous medium and thin films. The bridging coefficient is apart from Denkov et al.<sup>18</sup> not evaluated in most studies.

### 2.5.2 Lamella number

In order to predict foam stability in the presence of oil the E and S coefficients can be used. However, the oil droplets can only enter the foam lamella if they are smaller than the lamella. The (residual) oil in porous media may not contain droplets of that size. If this is the case, the oil droplets cannot enter the foam lamella, independent of the values of the E and S coefficients. The values of E and S are therefore not applicable to the prediction of foam oil interactions<sup>27,28</sup>. Emulsification of the oil is thermodynamically only favoured for negative values of the interfacial tension<sup>28</sup>. Negative interfacial tensions are impossible in nature, therefore spontaneous emulsification can not occur. Observations have shown, however, that emulsification in Plateau borders can occur<sup>28</sup>. The capillary forces that draw oil up into the lamella and a pinch-off mechanism, are responsible for this emulsification of the oil. The resistance of the oil against this force comes from the tendency of the oil to minimise its interfacial area, due to its interfacial tension with the aqueous solution. These two opposing effects can be determined as a dimensionless ratio, the lamella number:

$$L = \frac{\Delta P_C}{\Delta P_R} = \frac{\gamma_{GS} * r_o}{\gamma_{OS} * r_p} \quad (2.7)$$

were  $r_p$  is the radius of the plateau border and  $r_o$  is the oil drop radius. If the capillary suction,  $P_C$  is bigger than the resistance,  $P_R$  of the oil against this force, the lamella number will be bigger than 1. Values between 1 and 7 indicate that oil will be sucked into the lamella but the foam will remain semi stable. When L is greater than 7 an unstable foam will be obtained. The foam destruction in the lamella theory involves firstly the emulsification of the oil into small droplets and secondly the penetration of the droplets at the solution-gas interface thereby rupturing the lamella film. Schramm and Novosad<sup>28</sup> found experimentally that  $r_o/r_p = 0.15$ . This ratio is impossible to determine in core flooding experiments, therefore the value of 0.15 found by Schramm and Novosad is used in this study. Assuming a constant ratio formula 2.7 indicates that surfactant solutions with a high interfacial tension with the oil and a low surface tension will give the best foam in presence of oil according to the lamellae theory.

The lamella number defined by Schramm and Novosad<sup>28</sup> is based on observations in a micro model, and did predict foam oil interactions well in this situation. In core flooding experiments, the lamella number was found to have no predicting power about the foam stability at all, according to Andrianov et al.<sup>25</sup>, Bergeron et al.<sup>26</sup>, Dalland et al.<sup>21</sup>. Vikingstad et al.<sup>29</sup> investigated the lamella number in a bulk foam experiment, and conclude that the lamella number does not predict the stability of bulk foam in the presence of oil.

### 2.5.3 Pseudo-emulsion film

A pseudo-emulsion film is the film of surfactant solution between the oil drop and the gas phase, and can be an important factor for the stability of foam containing emulsified oil. The importance of this film in relation to foam stability was first observed by<sup>10</sup>.

Manlowe and Radke<sup>23</sup>, Koczko et al.<sup>30</sup>, Bergeron et al.<sup>26</sup>, Lee et al.<sup>22</sup> all agree on the importance of the pseudo emulsion film with respect to foam stability in the presence of oil. A negative generalised entering coefficient can be directly related to a stable pseudoemulsion film according to<sup>26</sup>. Lee et al.<sup>22</sup> and Koczko et al.<sup>30</sup> described two foam oil interactions, firstly the oil can be solubilised in the surfactant solution, in this case the foam will be unstable. Secondly emulsification occurs, and the stability of the foam depends of the stability of the pseudo emulsion films.

### 2.5.4 Summarised results of previous studies

The results of previous studies are summarised in table 2.1. The different stability criteria previously discussed are considered for three types of foam experiments, bulk foam, micro model and porous media. The work of different authors is presented in table 2.1 If the results of the experiments agree with the stability criteria there is a green box around the paper. If the stability criteria and the conclusions of a paper are contradictory the color of the box is red.

Stability criteria	Foam stability	Bulk foam	Micro model	Porous media
$E < 0$	Stable	Denkov et al. <sup>18</sup>		Dalland et al. <sup>21</sup> Bergeron et al. <sup>26</sup> Mannhardt et al. <sup>24</sup>
$B < 0$	Stable	Denkov et al. <sup>18</sup>		
$E > 0$	Unstable	Denkov et al. <sup>18</sup> Lau and O'Brien <sup>19</sup>	Manlowe and Radke <sup>23</sup> Koczó et al. <sup>30</sup>	Lee et al. <sup>22</sup> Dalland et al. <sup>21</sup> Kristiansen and Holt <sup>20</sup>
$B > 0$	Unstable	Denkov et al. <sup>18</sup>		Mannhardt et al. <sup>24</sup> Dalland et al. <sup>21</sup>
$L < 0$ $1 < L < 5.5$ $L > 5.5$	Stable Intermediate Unstable			Dalland et al. <sup>21</sup> Andrianov et al. <sup>25</sup> Bergeron et al. <sup>26</sup>
		Vikingstad et al. <sup>29</sup>	Schramm and Novosad <sup>28</sup>	
Stable pseudoemulsion film	Stable	Lee et al. <sup>31</sup> Nikolov et al. <sup>10</sup>	Koczó et al. <sup>30</sup> Manlowe and Radke <sup>23</sup>	Raterman <sup>32</sup>

TABLE 2.1: The work of different authors summarised. If the results of the author agree with the stability criteria the box is marked green, otherwise the box is red.

## 2.6 Foam in porous media

### 2.6.1 Mobility reduction

To improve the volumetric sweep of oil recovery processes that use gases, the gas can be injected with a surfactant solution to form foam. The volumetric sweep of foam is improved, because the mobility of foam is many orders of magnitude lower than the gas mobility<sup>33,34,35</sup>. The foam in a porous medium exists as a gas phase dispersed in a continuous liquid phase. The gas separated by lamellae occupies the bigger pore channels<sup>36</sup>. The wetting surfactant fills up the smallest pore channels, and coats the walls of the foam filled pore channels. The mobility reduction of the liquid phase is the result of the lower liquid saturation. Gas in the system reduces the liquid saturation, and therefore reduces the relative liquid permeability. For this effect there is no foam needed, the relative permeability function is equal for foam flow as for unfoamed gas flow<sup>37</sup>.

Large viscous stresses, in the liquid which coats the pore walls, and in the lamellae that separates the gas phase, create a pressure drop. Another effect is that not all the gas is flowing in the porous medium, the intermediate pore channels can be blocked by stationary gas, which also reduces the relative permeability<sup>38,1,35</sup>.

### 2.6.2 Foam generation in porous media

Foam is created in the subsurface by either simultaneous co-injection of a surfactant solution and gas, or by surfactant-alternating-gas(SAG) injection. During the injection of the surfactant solution and the gas, foam will be generated due to the geometry of the pores. The foam generation can be divided into three different mechanisms: Snap-off, lamella division and leave behind.

**Snap-off** The predominant foam generating mechanism in porous media is snap-off<sup>39</sup>. When gas travels through a pore-throat, coated with the wetting phase, the constriction can induce capillary snap-off and a bubble will be formed. An illustration of this mechanism is shown in figure 2.10.

**Lamella division** A single lamella can be split into two or more lamellae when there are multiple possible pathways for the lamella to enter. Figure 2.10 shows the geometry where this type of foam generating mechanism can occur, and how this mechanism works.

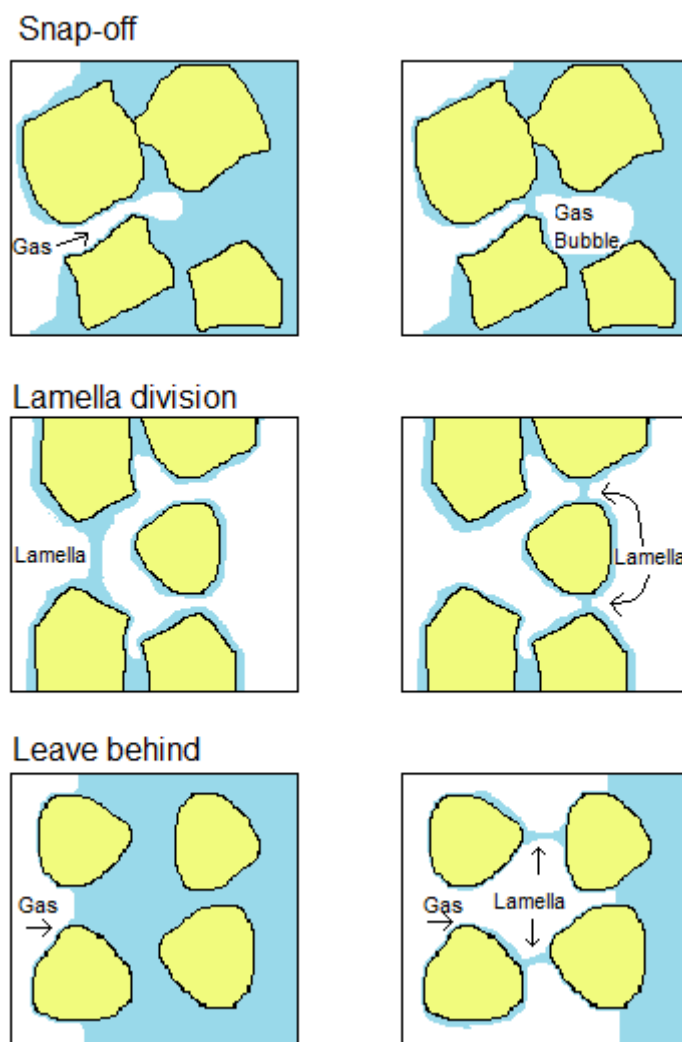


FIGURE 2.10: The three different foam generation mechanisms in porous media.

**Leave behind** When gas is displacing a surfactant solution, lamellae can be formed when the gas arrives simultaneously at a pore throat from two different directions (figure 2.10).

Lamellae generated by leave behind give approximately a fivefold reduction in gas permeability, while foams generated by the snap-off mechanisms can give several hundred fold gas permeability reduction<sup>39</sup>. In terms of permeability reduction snap-off is therefore a much more important mechanism.



### 2.6.3 Foam destruction in porous media

In porous media there are two mechanisms of foam coalescence, capillary suction and gas diffusion. Capillary suction is the most important mechanism, causing lamella breakage<sup>40</sup>. The coalescence rate of lamellae in porous media depends on the capillary pressure. As the liquid fraction decreases, the capillary pressure increases. This rise continues until a critical capillary pressure is reached, which lamellae can not withstand. Khatib et al.<sup>41</sup> named this value the limiting capillary pressure, it depends on the surfactant solution and the gas velocity. The permeability of the rock is also expected to be an important parameter.



## Chapter 3

# Bulk foam stability

### 3.1 Introduction

Bulk foam experiments were carried out with seven different surfactants to evaluate the effect of oil on the foamability and foam stability. There are different stability criteria that predict the effect of oil on foam stability. A study was performed to test the reliability of the predictions of the entering, spreading and bridging coefficients and the lamella number in bulk foam.

### 3.2 Experimental description

#### 3.2.1 Materials

For the bulk foam experiments dodecanol and six commercially available surfactants were used without any additional purification. Seven different solutions (detailed in table 3.1) were made with these surfactants. Two different types of AAS surfactants were used and therefore displayed as AAS 1 and AAS2. Four solutions contained a single surfactant, two solutions were a mix of two different surfactants and one solution contained a single surfactant and dodecanol. Dodecanol is not a surfactant, but has an effect on the behaviour of surfactants. The equilibrium absorption levels increase, resulting in a lower surface tension. The rate of micelle breakdown decreases, this means a slower transport of surfactants to the air-water interface<sup>42</sup>.

All the solutions contained 0.5 weight percent, wt%, of total active surfactant. For all the surfactants this concentration is well above the cmc. The surfactants were dissolved in a brine. This brine is prepared with demineralised water and 3 wt% sodium chloride.

Solution No.	Surfactant and concentration
1	IOS 0.5 wt%
2	AAS 1 0.5 wt%
3	AAS 2 0.5 wt%
4	AOS 0.5 wt%
5	AOS 0.25 wt% + IOS 0.25 wt%
6	AOS 0.25 wt% + Betaine 0.25 wt%
7	Betaine 0.5 wt % + Dodecanol* 0.005 wt%

TABLE 3.1: The type of surfactants used in the different solutions. (\*Dodecanol is a fatty alcohol).

The oil used to evaluate the foam stability was a paraffin oil, Isopar H, from ExxonMobil Chemical. A red dye (Sudan red from Sigma-Aldrich) was added to all the oil used, to make it better visible. This red dye has been used extensively in previous studies and is known not to change the properties of the oil. All the measurements and experiments are carried out with the dyed oil, to exclude the risk of working with oils that have different properties. The properties of the oil are listed in table 3.2.

Name	Chemical name	Density (55.0 °C) [kg/m <sup>3</sup> ]	Surface tension (55.0 °C) [mN/m]
Isopar H	Alkanes, C9-12-iso	732.87	18.64

TABLE 3.2: Properties of the used paraffin oil, Isopar H.

### 3.2.2 Solution stability

For all the surfactant solutions, the first thing that was evaluated was the solution stability. The surfactant solutions were stored at different temperatures (20°C and 55°C) for one week, and afterwards visually inspected. A clear solution without any undissolved particles indicated a stable solution. The first stability checks resulted in unstable solutions. The AOS surfactant that was initially considered, caused stability problems. Therefore it was replaced by another AOS surfactant. The final seven solutions were all clear at both temperatures, apart from solution 2 which had a slightly milky color, but this was considered to be acceptable.

### 3.2.3 Measurement of interfacial properties

The interfacial properties of the different solutions were measured at ambient temperature and at 55°C. The measurements at ambient temperature were performed using the pendant drop method. The profile of a drop of liquid suspended in another liquid or gas is determined. The shape of the drop is a balance between gravity and surface forces. The density of the liquids (surfactant solutions and Isopar H) and air were measured. Knowing these densities, the Krüss software can calculate the surface forces.

For the measurements at 55°C a spinning drop tensiometer was used. A rotating horizontal tube was filled with the more dense liquid, in this case the surfactant solution. A bubble of air, or a drop of oil was then placed in the tube with the surfactant solution. The tube was rotated to create a centrifugal force, the drop in the surfactant solution deformed to a more elongated shape. The centrifugal forces and the interfacial tension are in equilibrium when the shape of the drop is constant. The centrifugal forces can be found, knowing the speed of rotation. With this information the Krüss software can determine the surface or interfacial tension.

### 3.2.4 Bulk foam experimental set-up

The bulk foam experiments were performed using the commercially available Foamscan apparatus (figure 3.1). The Foamscan generates foam by sparging nitrogen through a glass frit, located at the bottom of a round glass tube. Before the experiment the tube was filled with a fixed amount of surfactant solution (50 ml). The foaming was started and continued until the desired volume of foam was reached (100 ml). The foam volume is optically monitored by a CCD camera during the generation and decay of the foam. The glass tube was double layered and connected to an external water bath. This made it possible to control the temperature in the tube. The tube was covered with a cap to prevent evaporation.

The main results acquired with the Foamscan set-up were the foamability and the foam stability. The foamability was determined by measuring the time necessary to reach the desired volume of foam. The foam stability was determined by measuring the half-life of the foam; this was the time needed to reduce the initial foam volume by 50% after the sparging was stopped.

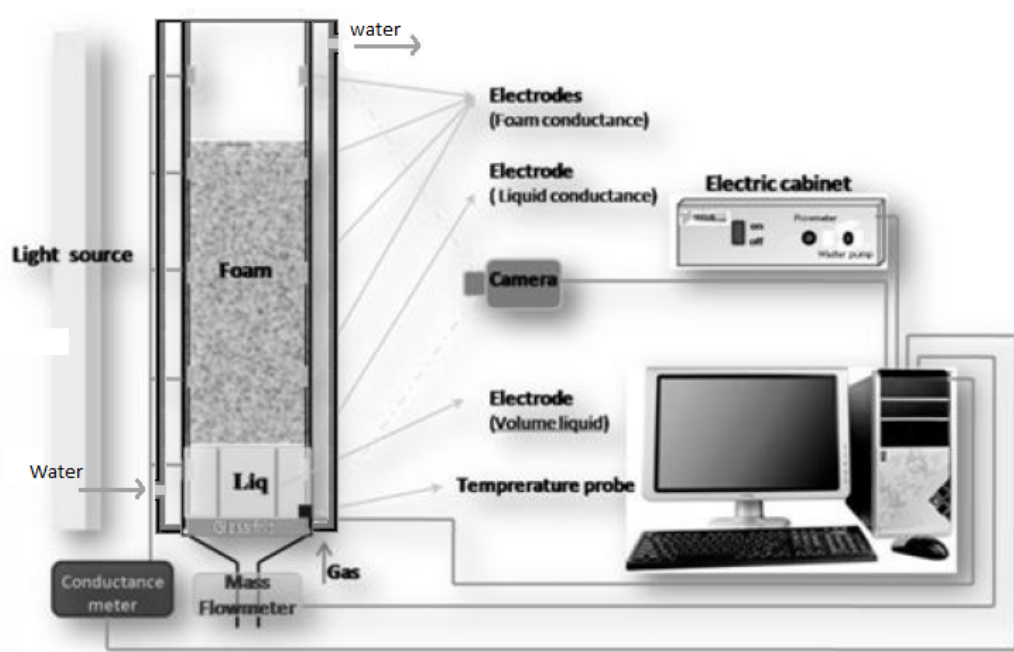


FIGURE 3.1: Schematic overview of the Foamscan device adapted from manufacturer TECLIS.

### 3.2.5 Experimental procedure

The bulk foam experiments were performed at 55°C and at atmospheric pressure. The surfactant solution was preheated to 55°C before it was placed in the Foamscan. The nitrogen was injected with a flow rate of 50 ml/min. For the experiments with oil 2.5 ml of oil, preheated to 55°, was added on top of the surfactant solution. After the oil was added the experiment was started immediately, to prevent the surfactant from equilibrating with the oil. All the experiments in the presence and the absence of oil were performed two times. If the results were doubted an extra measurement was performed.

After each test the Foamscan was thoroughly cleaned. The apparatus was partly dismantled and thoroughly flushed with tap water. Next the Foamscan was rinsed off with demineralised water and dried with air. If oil has been used, the paraffin oil was flushed out with ethanol first.

### 3.2.6 Bubble size measurement

In order to determine the average bubble radius and the polydispersity of the foam, samples were analysed under a microscope. The polydispersity index,  $\beta$  is defined as

the standard deviation of the radius of bubbles divided by the mean radius.

A sample of wet foam was taken direct after generation with the Foamscan apparatus. The foam was placed on a glass plate, and placed up side down under a microscope, because the microscope needs a flat surface to focus on (figure 3.2). The measured radius of the bubbles in a 2D cross section can differ from the real radius in 3D foam, because the bubble can be cut at different places. However, the results can be used to compare the foam generated with different surfactant solutions with each other.

The pictures of the samples were analysed with the image analysis software (ImageJ) in order to determine the size of the bubbles present in the sample.

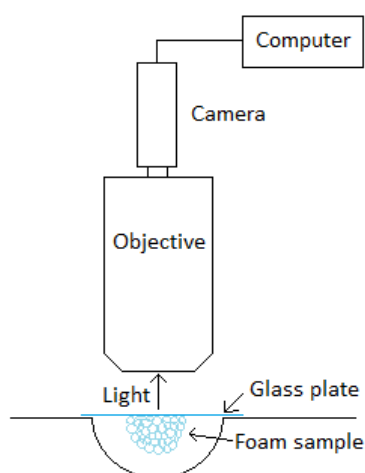


FIGURE 3.2: Schematic overview of the set-up, used to determine the bubble size.

## 3.3 Results

### 3.3.1 Interfacial properties

The measured surface tensions and interfacial tensions are listed in table 3.3. The surface tension decreases with increasing temperature. The interfacial tension also changes with temperature, but the change is surfactant dependent, in some cases it was decreasing and in some cases it was increasing.

Solution No.	SFT 20°C [mN/m]	IFT 20°C [mN/m]	SFT 55°C [mN/m]	IFT 55°C [mN/m]
1	27.15	0.33	22.80	0.31
2	26.54	0.56	20.50	0.60
3	26.75	1.27	25.00	0.61
4	28.77	1.00	21.50	1.18
5	27.96	0.49	22.00	0.47
6	27.25	0.58	23.90	1.27
7	26.74	1.59	21.80	0.67

TABLE 3.3: Interfacial properties of the surfactant solutions at 20°C and 55°C (SFT is the surface tension with air and IFT is the interfacial tension with Isopar H).

### 3.3.2 Foamability

The foamability is the ease with which foam is produced by agitation. This is evaluated by measuring the sparging time needed to create 100 ml foam. The foamability of the surfactant solutions with and without oil are shown in table 3.4.

Solution No.	Average foaming time without oil [s]	Standard deviation	Average foaming time with oil [s]	Standard deviation
1	106.58	4.23	139.91	17.829
2	105.26	2.69	126.87	11.18
3	108.08	1.46	117.79	0.34
4	106.32	3.49	112.34	2.05
5	102.80	9.03	112.18	6.69
6	108.28	1.59	121.99	4.52
7	108.32	2.68	125.40	1.80

TABLE 3.4: Average time (n=2) needed to get 100 ml foam, with and without oil.

### 3.3.3 Bubble size

A foam sample was analysed for all the solutions tested, except for solution 2. The foam samples (figure 3.3) were generated with the Foamscan apparatus at an equal gas flow rate. The difference in average bubble size was relatively small (table 3.3). The polydispersity index shows that the foams were fairly polydispersity.



Solution No.	Average bubble radius [mm]	SD [mm]	$\beta$ [-]
1	0.170	0.066	0.39
3	0.191	0.068	0.36
4	0.174	0.066	0.38
5	0.199	0.080	0.40
6	0.184	0.059	0.32
7	0.202	0.070	0.35

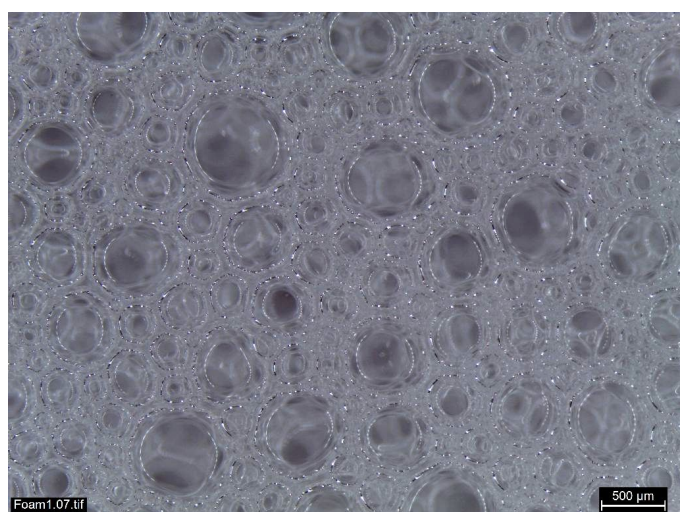
TABLE 3.5: The mean bubble radius, the standard deviation and  $\beta$  of the different solutions tested.

### 3.3.4 Bulk foam stability

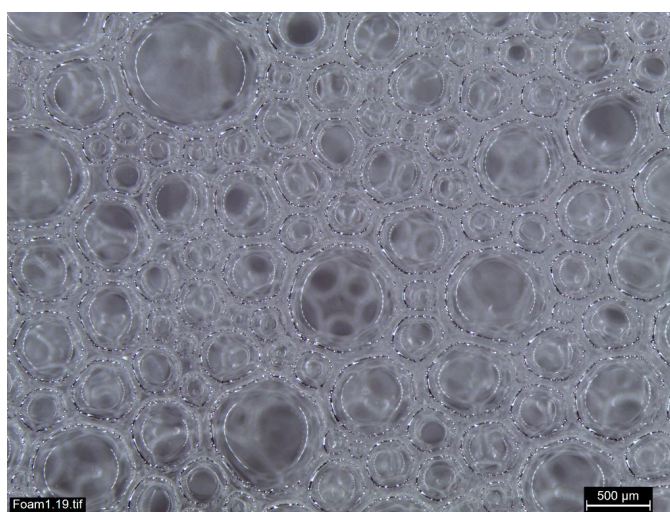
The stability of the foam generated with seven different surfactant solutions is evaluated. Figure 3.4 shows the half-life of the bulk foam experiments, both in the absence and presence of oil. A longer half-life indicates more stable foam. The conditions in which the foam is generated are equal for all the experiments, therefore the longer half-life can be dedicated to the type of surfactant. Solution 4 produced the most stable foam in the absence of oil, solution 1 produced the least stable foam. The error bars show the calculated standard deviation. The results obtained with the Foamscan apparatus are reproducible.

The extent to which the oil decreases the foam stability depends on the surfactant used. All the surfactant solutions perform systematically worse in the presence of oil (figure 3.4). Solution 4 performs best without oil, but when oil is introduced there is a big reduction in stability. In comparison, solution 3 does not perform very well in the absence of oil, but the stability is only slightly reduced in the presence oil. It was found that the most stable foam in the presence of oil is produced with solution 6.

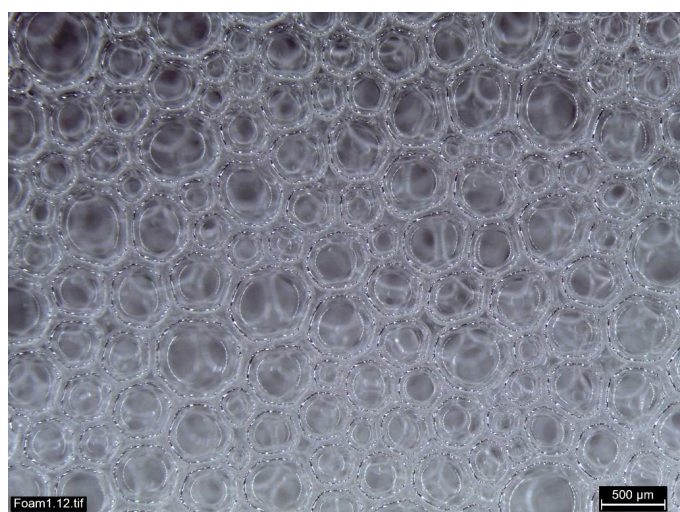
The range of the error bars is small for most of the surfactants. There is a large variation in the half-life of solution 3 in the presence of oil. This variation can be attribute to the way the foam collapsed. For this surfactant, destabilisation by the oil causes large foam collapse events. There is a variation in when these occur, and this results in scatter in the values of half-life of the foam. The foam volume curve for three experiments with solution 3 in the presence of oil are shown in figure 3.5, demonstrating the range of collapse behaviours observed.



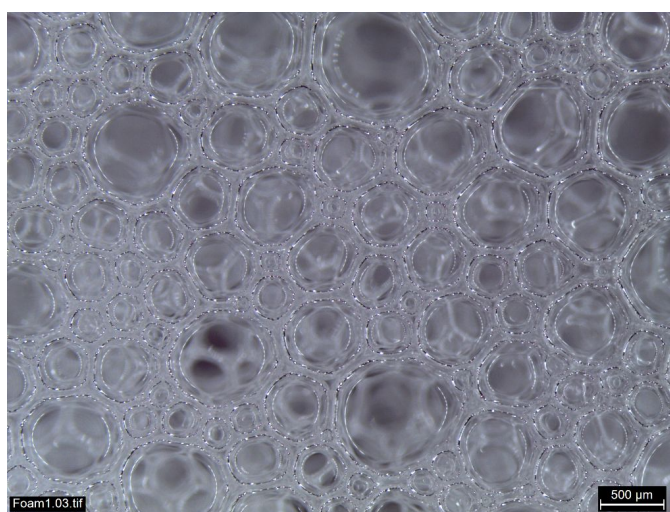
(A) Solution 1



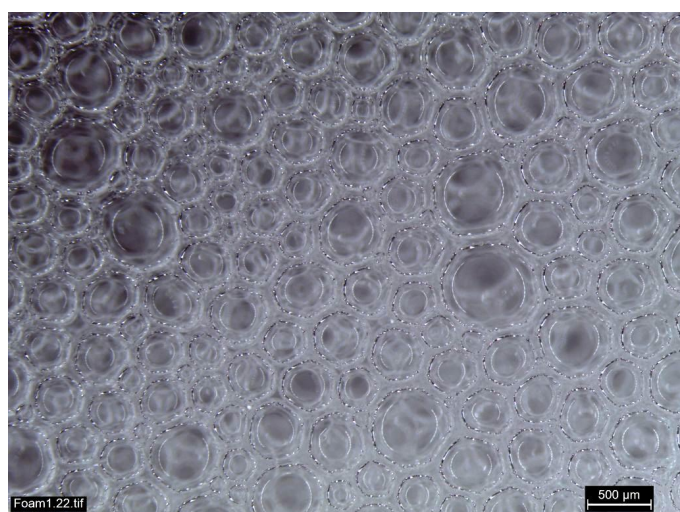
(B) Solution 3



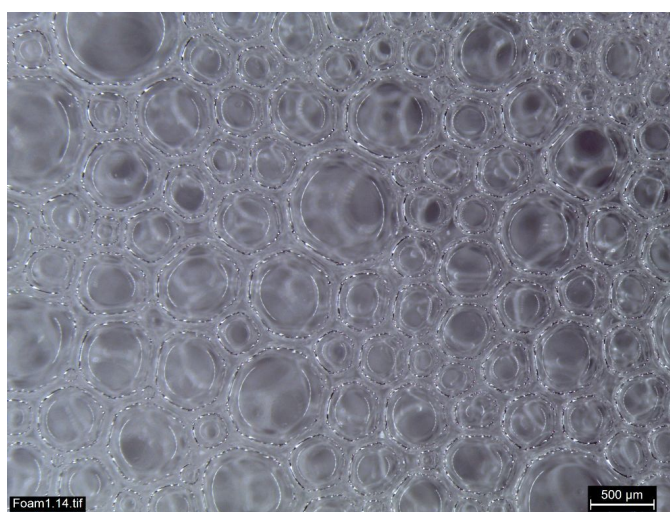
(C) Solution 4



(D) Solution 5



(E) Solution 6



(F) Solution 7

FIGURE 3.3: Samples of wet foam generated in the Foamscan for each surfactant solution. The foams are polydisperse, but the range of bubble sizes is fairly consistent for all the samples studied.

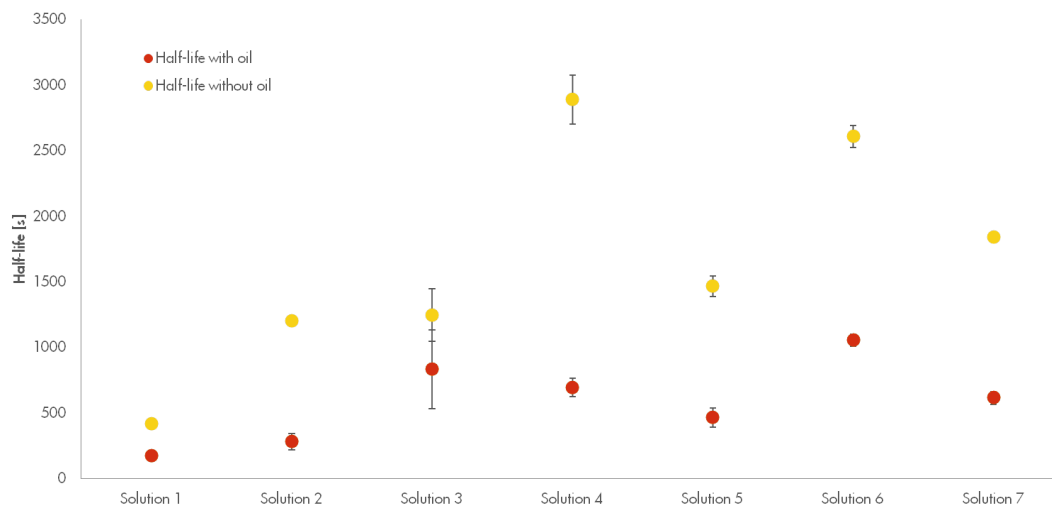


FIGURE 3.4: The average ( $n=2$ ) half-life of the seven different solutions in the absence and the presence of oil.

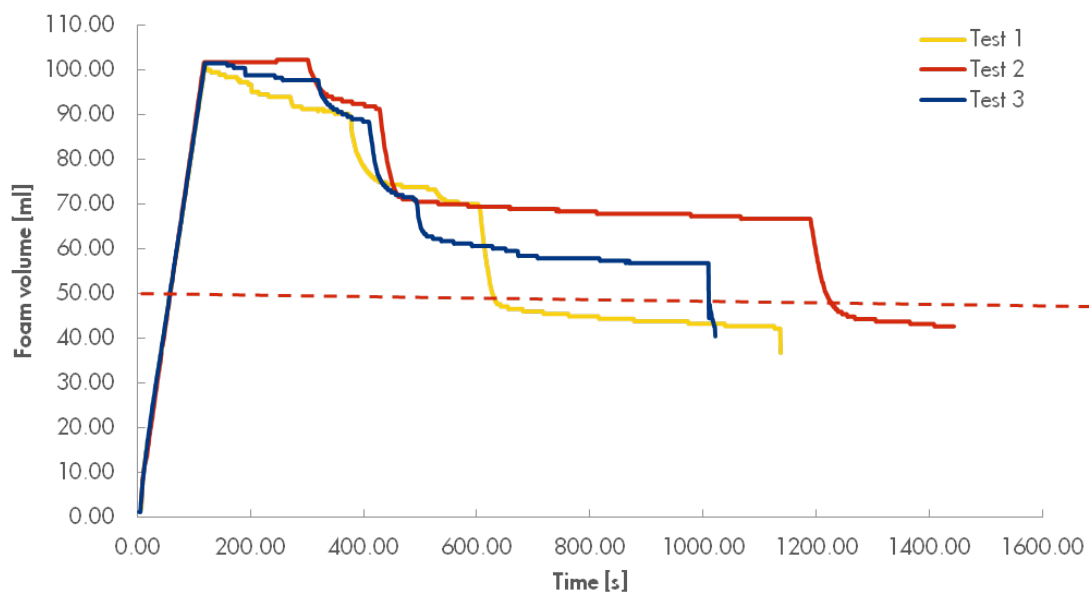


FIGURE 3.5: The foam volume plotted over time for three bulk foam experiments with solution 3 in the presence of oil.

Solution No.	E	S	B	L	Half-life* [s]
1	4.47	3.85	172.49	11.03	177.25
2	2.46	1.26	73.16	5.13	281.65
3	6.97	5.75	277.92	6.15	834.74
4	4.04	1.68	116.19	2.73	695.41
5	3.83	2.89	136.77	7.02	467.63
6	6.53	3.99	225.37	2.82	1056.82
7	3.83	2.49	128.24	4.88	617.27

TABLE 3.6: The different coefficients and the lamella number for all the surfactants. Green indicates the best, and red the worst (predicted) performance \*Half-life in the presence of oil.

### 3.3.5 Stability criteria

As mentioned in chapter 2, there are several different stability criteria for foam, stabilised by one or more types of surfactant in the presence of oil. The entering E, spreading S and bridging B coefficients and the lamella number, L were calculated using the measured interfacial properties. Table 3.6 shows the values for all the solutions used.

The obtained values of the coefficients and the lamella number give an insight into foam stability in presence of oil. As can be seen in table 3.6 all the values give a positive entering coefficient, which means that it is favourable for the oil to enter the solution-gas interface. The positive spreading and bridging coefficients indicate that oil will spread and will not be able to form stable bridges.

## 3.4 Discussion

### 3.4.1 Foamability

The differences in foamability are relative small compared to the standard deviation. This makes comparison of foamability between the surfactants difficult. Foam generation is in this case not surfactant related, but depends on the generation method. A lower gas injection rate, is expected to result in a bigger differences in foamability. When oil is present the time needed to create 100 ml foam is significantly longer. Table 3.4 does clearly show that the oil has a negative effect on the foamability.

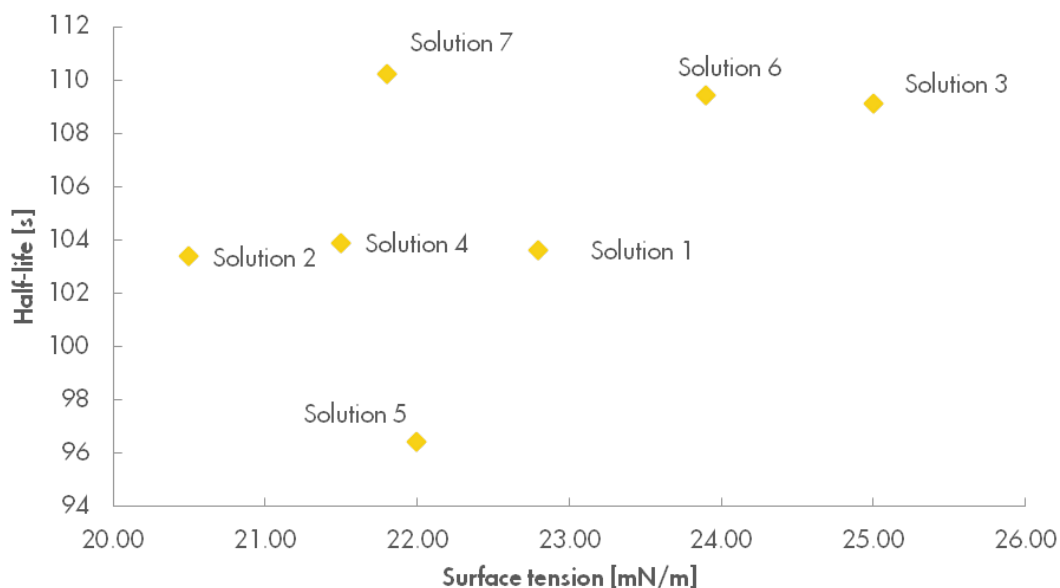


FIGURE 3.6: The half-life of the foam in the absence of oil is plotted against all the associated surface tension for all the solutions tested.

### 3.4.2 Surface tension

In order to create foam, a surfactant needs to lower the surface tension. A lower surface tension lowers the total energy of the system. However, no correlation between foam stability and surface tension is found. (figure 3.6). It is therefore not possible to predict how different surfactants will perform as a foaming agent based on the surface tension alone.

### 3.4.3 Entering, spreading and bridging coefficient

The combination of oil and surfactant solutions used, resulted in positive entering coefficients for all solutions. Therefore, it is not possible to conclude if a negative entering coefficient results in stable foam. All the solutions tested produced foam that was destabilised by the oil as predicted by the positive entering coefficient. However, it is observed that the magnitude of  $E$  does not correlate with the stability of the foam.

The  $E$  coefficient determines if it is favourable for the oil to enter the surface or not, but does not predict the time needed to enter. This makes the  $E$  coefficient an unreliable tool to predict foam-oil interaction. The entering coefficient is unreliable, because it does not take thin film forces into account. This is described by Denkov et al.<sup>18</sup> as the entry barrier. The surfactant layer at the interface can form a barrier that is hard to penetrate for the oil droplets, which is due to the surfactant molecules<sup>26</sup>. Therefore predictions

for positive entering coefficients are unreliable, notwithstanding that a negative entering coefficient should result in a stable foam.

All the oils are spreading ( $S > 0$ ) and are not able to form stable bridges ( $B > 0$ ). Therefore it is impossible to conclude if these coefficients are reliable as foam stability predictors. All the solutions tested produced foam that was destabilised by the oil as predicted by the positive spreading and bridging coefficients. The magnitude of  $S$  and  $B$  does not correlate with the stability of the foam.

#### 3.4.4 Lamella number

The lamella number does predict correctly the best and worst performing solutions in the presence of oil. For the intermediate solutions it is not possible to observe a correlation between the lamella number and the foam stability. One reason why the lamella number is not reliable, could be the adapted value of the ratio of the radii  $r_o/r_p = 0.15$ , which was determined in a micro model. This value may vary significantly for bulk foam.

Another possibility why the lamella number is not reliable is because this number determines if a single lamella can emulsify oil. In these type of bulk foam experiments introduction of oil in the lamella by emulsification due to suction can be less important, because there is already oil in the foam, due to the foaming process.

#### 3.4.5 Interfacial tension

The interfacial tension between the oil and the surfactant solutions shows a clear link with foam stability (figure 3.7). A higher interfacial tension results in a foam that decays slower. This effect could be due to the method used to create foam. Before the foaming started the oil was floating as a layer on top of the surfactant solution. As the foaming started the first foam films contain a lot of oil, the amount of oil is reduced when a gap is formed in the middle of the oil layer. The amount of oil transported upwards with the first foam bubbles depends on the interfacial tension of the oil with the surfactant solution. A lower interfacial tension results in more oil in the foam, and this higher oil concentration accelerates the foam decay. By carrying out the experiment this way, the amount of oil present in the foam depends on the interfacial tension and is therefore not equal for every surfactant solution.

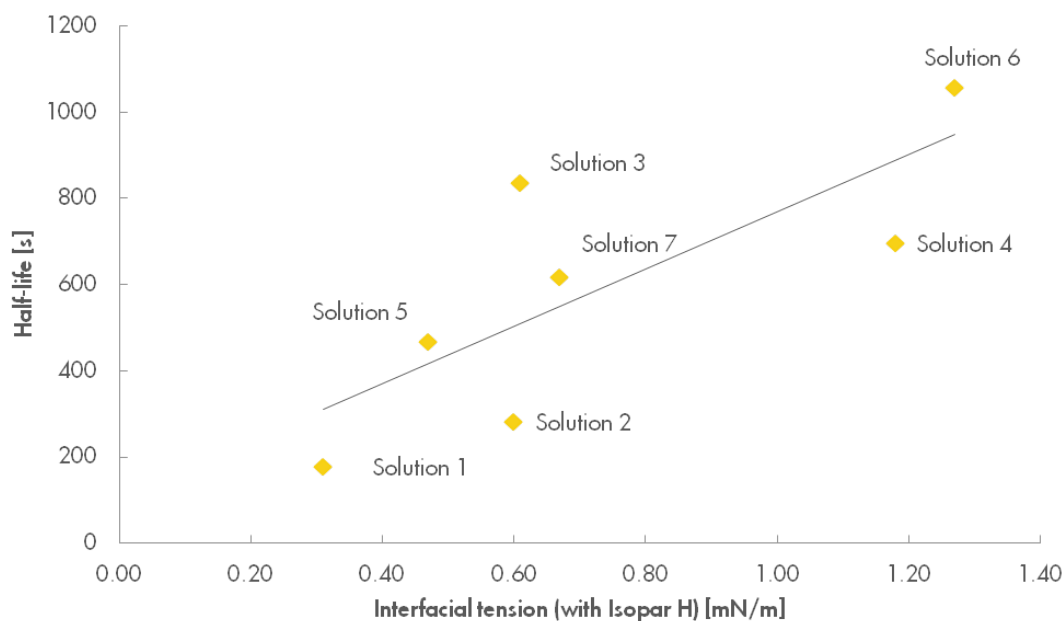


FIGURE 3.7: A plot of the foam half-life as a function of the interfacial tensions of the surfactant solution with Isopar H.

### 3.5 Conclusions

A range of bulk foam experiments were performed with seven different surfactant solutions. The stability of the foam in the presence and in the absence of oil was analysed. All the experiments were performed at 55°C and atmospheric pressure, and were repeated at least twice. The following conclusions can be drawn from these experiments:

- The oil destabilises the foam for every surfactant solution used. The reduction in stability is surfactant dependent.
- The negative entering coefficient did predict the unstable foam in the presence of oil. The entering coefficient is not useful as a tool to predict the stability of foam in the presence of oil, because it does not predict when the oil enters the gas-liquid interface. This is probably because the thin film forces are not taken into account. Thin film forces only influence the positive entering coefficient, so for a negative entering coefficient the predictions could be useful.

With this combination of oil and surfactants, it is impossible to conclude anything about the usefulness of the spreading and bridging coefficients. In all cases the calculated values of  $S$  and  $B$  were both positive which would indicate an unstable foam and these were observed. No cases of  $S < 0$  and  $B < 0$  and stable foam were observed.

- 
- The lamella number has a weak predicting value in bulk foam, probably because of the differences between the lamellae in the bulk foam and the lamellae in the micro model where  $L$  was originally defined.
  - There is a clear correlation between the half-life of the foam in the presence of oil and the interfacial tension. This effect may be caused by the amount of oil that is transported up with the foam column during foaming. A lower interfacial tension between the oil and surfactant indicates that more oil will be carried up during the foaming process. The interfacial tension gives the best indication of bulk foam stability in the presence of oil in this study.



## Chapter 4

# Foam in porous media

### 4.1 Introduction

Core flood experiments were performed to evaluate the performance of different types of surfactants in a porous medium. The porous medium used was a natural sandstone. Gas and surfactant solution were co-injected in different ratios and the foam was generated in the core. The pressure drop over the core was the main criteria used to judge the performance of the foam.

### 4.2 Core flooding theory

The gas and surfactant solution can be co-injected in different ratios. The gas fraction of the injected solution is called the foam quality,  $f_g$ :

$$f_g = \frac{q_g}{q_g + q_w} \quad (4.1)$$

where  $q_g$  the volumetric gas flow rate and,  $q_w$  the volumetric liquid flow rate. The pressure drop over the core is dependent on both the liquid and gas velocities. Figure 4.1 shows an example of the pressure gradient contours as a function of the liquid and gas velocity. The contour plot can be divided into two distinct regimes: The low quality regime in which the apparent viscosity is dependent on the gas flow rate (horizontal contours) and the high quality regime, where the apparent viscosity is only dependent on the liquid flow rate (vertical contours). The two regimes are separated by the line that marks the transition foam quality  $f_g^*$ .

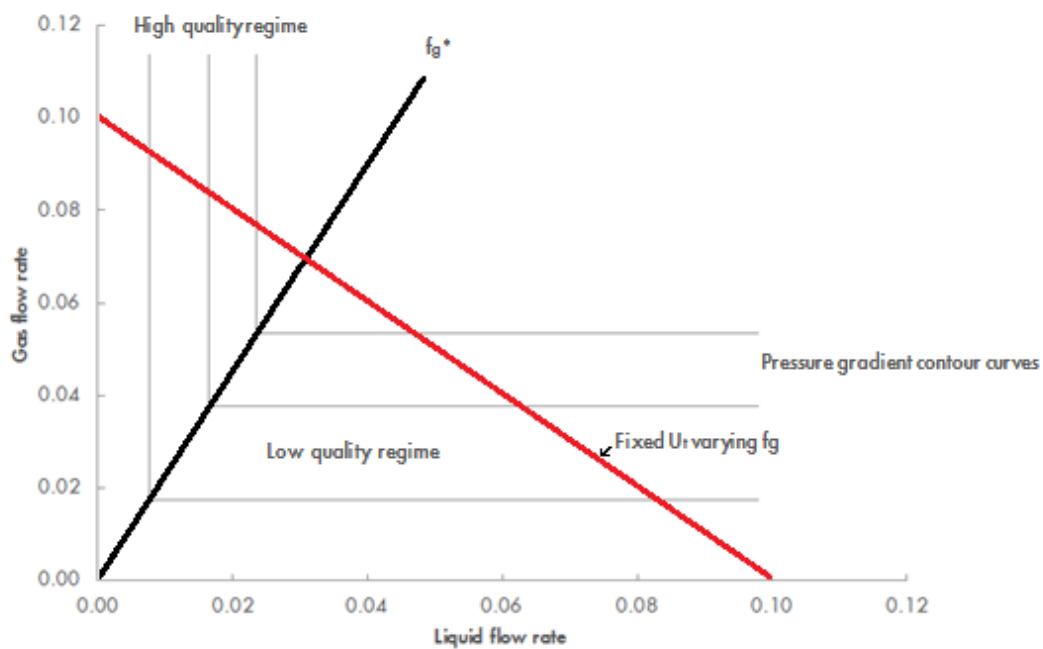


FIGURE 4.1: A schematic representation of the pressure gradient contours as a function of the liquid and gas velocity

To enable better comparison between different core flood experiments, the apparent viscosity of the foam in the core was considered instead of the pressure drop. The apparent viscosity of the foam in the core was obtained using the Darcy formula:

$$\mu_{app} = \frac{k}{u_t} \frac{\Delta P}{l} \quad (4.2)$$

in which  $k$  is the permeability of the core,  $u_t$  the total Darcy velocity  $\Delta P$  the pressure difference over the core and  $l$  the length of the core.

Figure 4.2 shows an example of a curve of the apparent viscosity obtained with a fixed total velocity and varying liquid fractions. The highest apparent viscosity, the peak in figure 4.2, occurs at  $f_g^*$ . To the left of the peak is the low foam quality regime where the flow is influenced by bubble trapping and release. To the right of the peak is the high quality regime, which is dominated by coalescence.

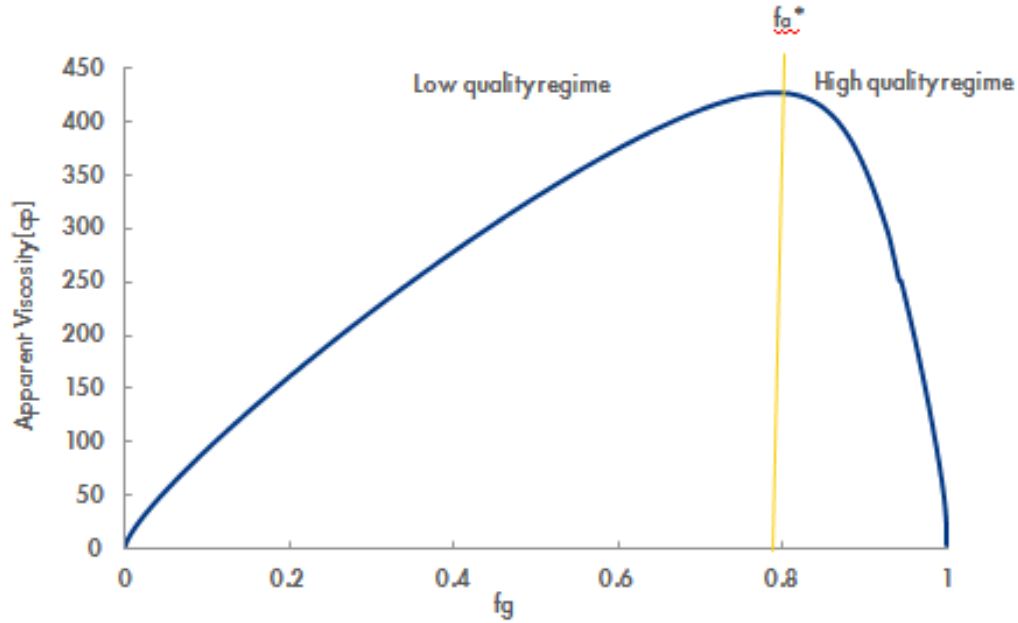


FIGURE 4.2: An example of a curve obtained with a fixed total flow rate

In the low quality regime the bubble size is assumed to be fixed, because diffusion causes bubbles smaller than the pore size to disappear<sup>43</sup>. Alvarez et al.<sup>44</sup> did observe a fixed bubble size in the low quality regime in their experiments. With a fixed bubble size, the pressure drop over the core is primarily dependent of the pore geometry and surface tension<sup>45</sup>. The surface tension does not vary greatly with different surfactant solutions, therefore the pressure drop in the low quality regime should not vary with different surfactant solutions.

## 4.3 Experimental description

### 4.3.1 Materials

The core flood experiments were performed with six different surfactant solutions. These solutions were identical to the solutions used for the bulk foam experiments, except that solution 2 was not used. The core floods were not performed with solution 2, because from visual inspections a slightly milky solution was observed, which indicated the presence of particles. These particles could clog and damage the core. The gas phase used for this experiment was nitrogen.

### 4.3.2 Core and core holder

The core flood experiments were performed using a Lilliput core. This is a core with a relatively small volume compared to the standard size cores normally used for flooding experiments. Using such a small core for core flooding experiments is a new technique and still in development. It has the advantage of being economical both in time and resources. The cores used for the tests were Bentheimer sandstone, an analogue reservoir rock. The properties of the cores are summarised in 4.1. The core holder was an aluminium tube. The core was placed in the holder and glue was injected to keep the core in position and to prevent fluid from bypassing along the side of the core. To prevent the injected glue from penetrating deep into the porous core, therefore the core was encapsulated in a thin layer of glue before placed into the core holder. An estimation of the effective area, and hence effective core diameter, was made using a micro-CT image of the core. The pore volume (pv) is the calculated void space in the core, based on a porosity of 23%. This number was determined in previous studies with Bentheimer sandstone cores drilled from the same block. The permeability of the core was determined from the measured pressure drops at different flow rates for single-phase surfactant solution flow.

Length [cm]	Effective diameter [cm]	Porosity [%]	Pore volume [cm <sup>3</sup> ]	Permeability [D]
17.0	0.94	23.0	2.7	1.8-2.1

TABLE 4.1: Properties of the used Bentheimer sandstone core used for the liliput core flood tests.

### 4.3.3 Experimental set-up

To effectively perform core flooding experiments on the Lilliput core, the volume of the set-up (pipes, connectors ect.) was kept as low as possible. Figure 4.3 shows a schematic overview of the set-up. The surfactant solution was injected at the bottom of the core using a double piston displacement pump. The nitrogen gas was supplied from a 200 bar cylinder, with the pressure reduced to 40 bar by the pressure regulator. A mass flow controller regulated the gas flow before injection at the bottom of the core. The pressure was measured in two places. The first measurement point was located in the liquid line, before the junction where the gas and liquid lines come together. The second measurement point was located at the outlet of the core, before the back pressure regulator. The difference in these pressure measurements gave the pressure drop over the core.

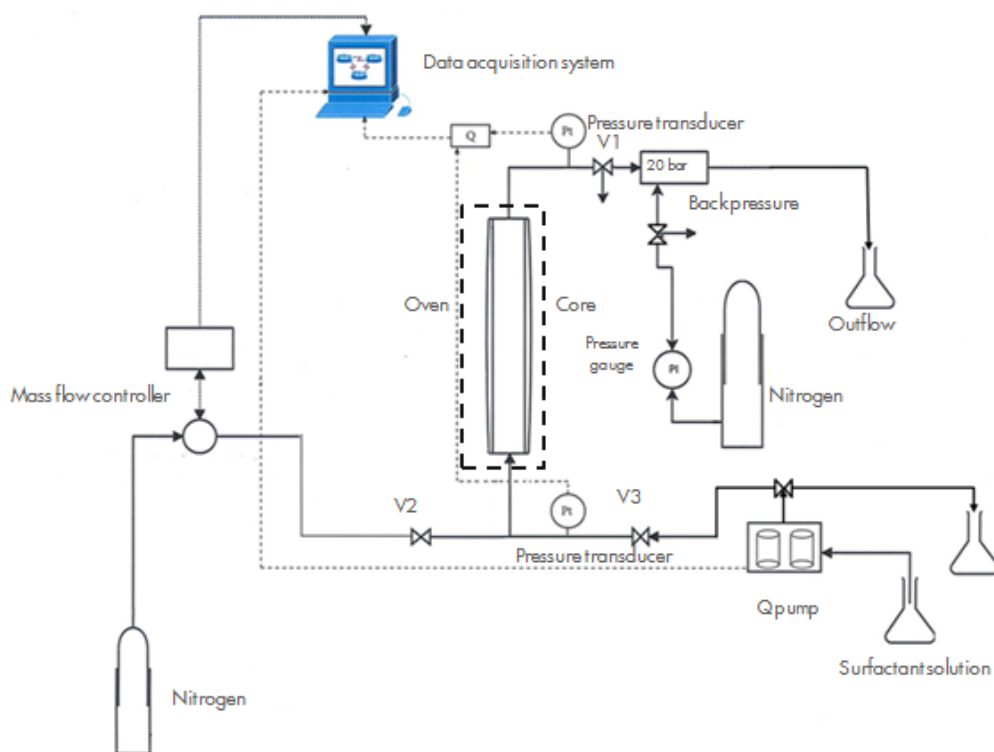


FIGURE 4.3: Schematic diagram of the Lilliput core flood set-up.

The pressure at the outlet of the core was controlled by a back pressure regulator. The experiments were conducted with a back pressure of 20 bar. Several spring loaded back pressure regulators were tested with this set up. These were of interest, because of their very small dead volume. Unfortunately these regulators could not cope with the two phase flow and were unable to keep the back pressure constant. Therefore a locally modified dome loaded back pressure regulator with a dead volume of approximately 1 ml was used. All the experiments were performed at 55°C, The temperature was regulated by placing the core in an oven.

#### 4.3.4 Experimental procedure

##### 4.3.4.1 Initial core set up

After placing a core into the set-up the following procedure was carried out:

1. Valve V1 (figure 4.3) was closed and a initial leak test was carried out with helium from the central line in the laboratory (8 bar).

2. Nitrogen from the cylinder was used to fill the system to 20 bar over pressure, the system was then sealed and a leak test was performed. When there were no significant leaks in the system, the pressure build-up was used to determine the total volume of the system.
3. To remove the nitrogen the system was flushed with CO<sub>2</sub> without back pressure. A vacuum pump was then used to remove the CO<sub>2</sub> from the system. When the pressure was constant, the system was filled with brine.
4. A back pressure of 20 bar was then put on the system and several pore volumes of brine were injected to dissolve and remove any CO<sub>2</sub> that remained in the system.

#### 4.3.4.2 Core flood procedure

The first six core flood experiments in the absence of oil were all performed on one single core. For the six different surfactant solutions their performance was determined by a foam quality scan. The experiments were performed at a fixed total flow rate,  $U_t$  with a varying foam quality,  $f_g$ . The gas and surfactant solution were co-injected to generate foam in the porous medium at a fixed superficial velocity of 6.75 ft/day. The injected volume of gas is pressure dependent; before the start of the experiment the pressure drop over the core was predicted, based on results of previous experiments and the flow rate was adjusted to that value.

The following procedure was repeated for every new surfactant solution tested in the same core:

1. 5 pv of surfactant solution was injected to displace the brine and let the core absorb the surfactant.
2. Nitrogen gas and surfactant solution were co-injected for at least seven different foam qualities.
3. 8 pv of foam killer (a mixture of 50% isopropanol and 50% demineralised water) was injected to break the foam and remove the surfactant molecules from the core.
4. 10 pv of brine was injected to flush out the foam killer.

## 4.4 Results

Figure 4.4 shows the results of a core flood experiment, this shape is typical for all pressure data obtained. The graph shows the pressure difference over the core versus

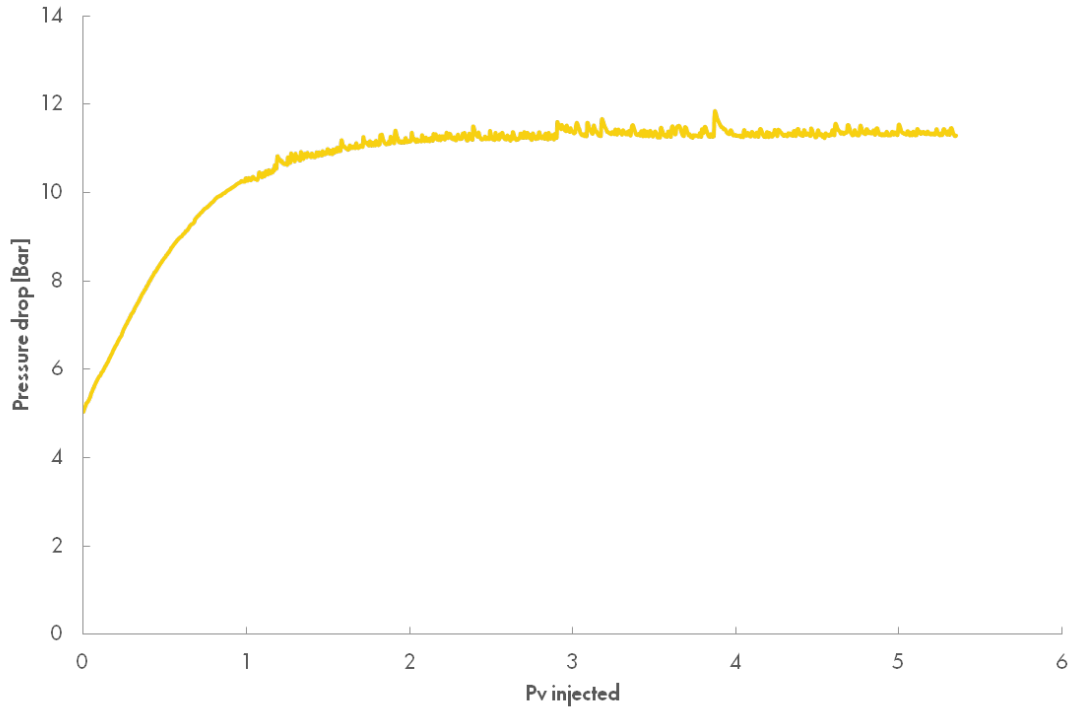


FIGURE 4.4: The pressure drop over the core versus the number of pore volumes injected. (This curve was obtained with solution 7 at  $f_g = 0.30$ )

the number of pore volumes of gas and surfactant solution injected. After 2.5 pv the pressure drop over the core became stable.

After the experiments the actual flow rate and foam quality was back calculated, based on the pressure in the middle of the core, assuming a constant pressure gradient over the core. Table 4.2 shows the maximum apparent viscosity for each surfactant solution with the associated foam quality. The maximum pressure gradient over the core measured is also listed. Appendix A contains the measured pressure gradient and apparent viscosity of the all the solutions. The surfactant solution that produced the most stable bulk foam, solution 6, was responsible for the highest apparent viscosity in the core flood experiments.

Figure 4.5 shows typical foam quality scan curves, i.e. a plot of the apparent viscosity versus the foam quality for four solutions. There are no significant differences in apparent viscosity between the surfactants solutions when  $f_g < 0.70$ . As the foam quality rises, more pronounced differences are observed between the surfactant solutions.

Solution No.	$Max\mu_{app}$ [cP]	$f_g^*$ [-]	$ \nabla P $ [Pa/m]
1	487	0.78	$52.5 \cdot 10^5$
3	504	0.74	$57.5 \cdot 10^5$
4	855	0.97	$89.7 \cdot 10^5$
5	741	0.89	$79.8 \cdot 10^5$
6	925	0.97	$96.5 \cdot 10^5$
7	750	0.89	$74.5 \cdot 10^5$

TABLE 4.2: Summary of the highest pressure gradient and apparent viscosity measured,  $f_g^*$  indicates the foam qualities at which these maxima occurred.

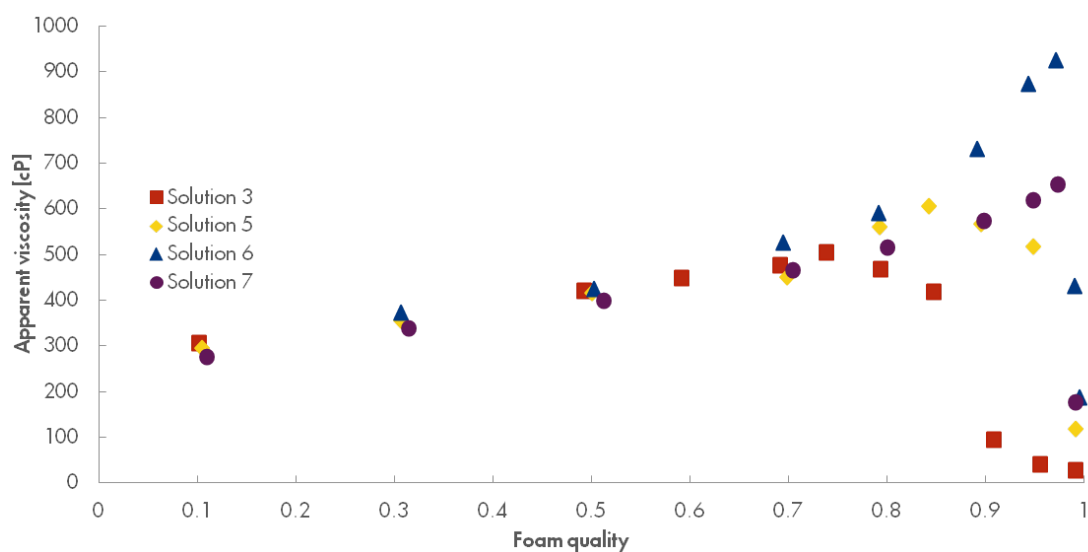


FIGURE 4.5: Foam quality scan curves, obtained with four different surfactant solutions.

## 4.5 Discussion

### 4.5.1 Set-up

This is the first study in which a Lilliput core has been used to do a foam quality scan. Good quality results were obtained with this small core, and it is suggested that it can be used as a good new surfactant screening tool. The Lilliput core is economical both in time and resources, which is a great advantage.



### 4.5.2 Experimental results

The results show that for foam qualities up to  $f_g = 0.70$ , all the surfactant solutions perform equally. At higher foam qualities in the low quality regime, differences in apparent viscosity were observed. This is contradicting with the idea that the pressure gradient is not related to the surfactant formulation in the low-quality regime. It is possible that the surfactant type alters the wall friction of lamellae in the low quality regime or that the apparent viscosity is affected by surface-tension gradients.

Interfacial rheology measurements were performed (more information can be found in Appendix A) and a difference in the loss (viscous) surface dilatational modulus was found between solutions 6 and 7. Both solutions are stable up to approximately the same foam quality, but there was a big difference in their performance in the low quality regime. Solution 6 had a higher elasticity and performed better in the low quality regime compared to solution 7. It could be possible that the higher surface viscosity is correlated to the density of the molecule adsorbed<sup>46</sup>. Golemanov et al.<sup>46</sup> suggest that the density of the molecules adsorbed is correlated to the film stability. A solution with a higher surface viscosity creates more elastic foam films. This should result in less film collapse and therefore generate a higher pressure drop over the core. The surface viscosity is dependent on the shear rate which is at this moment not well understood. Further experiments are needed to study this effect.

From the results of the core flood experiments (figure 4.5) can be observed that the apparent viscosity keeps increasing until  $f_g^*$  is reached, the high quality regime is entered and the apparent viscosity starts to decrease. The foam quality at which the high quality regime is entered is surfactant dependent. For surfactant screening and design it is valuable to have a good understanding of the surfactant solution properties that are important for the performance in the core.

When the gas fraction increases, the capillary pressure in the core rises<sup>41</sup>. The capillary pressure depends on the water saturation and will increase when the water saturation decreases. Foam filled pore channels and water filled pore channels exist together. Increasing the injected foam quality reduces the number of water-filled pores<sup>47</sup>. The capillary pressure will increase until the critical capillary pressure is reached, from this point on the capillary pressure is constant and the high quality regime is entered. In the high quality regime, foam behaviour is dominated by coalescence and the lifetime of the lamellae is exceedingly short<sup>41,48</sup>.

The capillary pressure in the core is equal to the capillary pressure in the lamella. In chapter 2 is discussed how the relative flat lamellae and the curvature of the Plateau border walls cause a pressure difference in the liquid phase. In the core is the difference

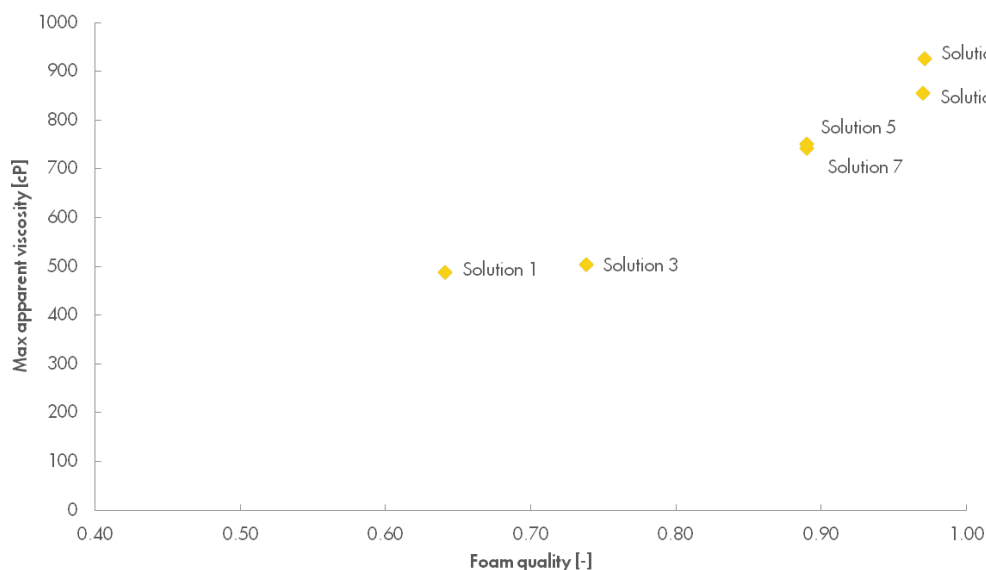


FIGURE 4.6: The maximum apparent viscosity plotted as a function of  $f_g^*$  (from the data in table 4.2).

between the radii determined by the capillary pressure. For stable films the capillary suction is in balance with the disjoining pressure. This would suggest, that disjoining pressure can be a very important criteria in surfactant screening and surfactant design.

The maximum apparent viscosity occurs at a different foam qualities for every solution. Plotting the maximum apparent viscosity against  $f_g^*$  (figure 4.6) shows that there is a link between the maximum apparent viscosity and  $f_g^*$ . If the foam is stable at higher foam qualities the apparent viscosity is higher as well.

### 4.5.3 Rheology in the low quality regime

In the low quality regime a shear thinning behaviour was expected, because both the yield stress of foam and the rheology of moving bubbles imply a shear-thinning behaviour<sup>45</sup>. The results obtained with the Lilliput set-up indicate a shear thickening rheology. It could be that this behaviour is a result of considering only the pressure drop measurement over the whole core, with the foam generating zone and capillary end effect included. These effects can be important, for example, the zone where the foam is generated becomes smaller the pressure drop over the core can becomes bigger even with a shear thinning rheology. Pressure taps in the core could be added to give more insight into the rheology behaviour of the foam in the core.

## 4.6 Conclusions

Core flood experiments were performed with six different surfactants in a Bentheimer sandstone core. Foam quality scans were obtained for each surfactant solution. The main conclusions of this study are listed below:

- The Lilliput core flow set-up is a good surfactant screening tool. The biggest advantage of a Lilliput core over a normal sized core is that less time and material is needed to do a core flood experiment.
- All the surfactant solution have the same apparent viscosity for foam qualities up to  $f_g = 0.70$ . The pressure drop over the core is not surfactant related. At higher foam qualities big differences in performance were observed between the solutions. The apparent viscosity can be affected by surface-tension gradients, it is suggested that more elasticity of the foam films result in a higher apparent viscosity. More experiments are needed to study this effect.
- There is a clear relation between  $f_g^*$  and the maximum apparent viscosity. A higher  $f_g^*$  generally resulting in a higher maximum apparent viscosity. The films collapse at a critical capillary pressure, for stable films the capillary suction is in balance with the disjoining pressure.



## Chapter 5

# Foam in porous media in the presence of oil

### 5.1 Introduction

The same experiments as in the previous chapter were repeated, only this time in the presence of oil. The results of the foam quality scans in the absence and presence of oil are compared. The different stability criteria of foam in the presence of oil (E, S, B coefficient and lamella number) are evaluated for foam in porous media.

### 5.2 Experimental description

#### 5.2.1 Materials and experimental set-up

The core flood experiments in the presence of oil were performed with the same surfactant solutions as used in the core flood experiments in chapter 4. Again Bentheimer sandstone cores were used, the geometry of the cores were not changed. The cores were saturated with Isopar H, the oil used in the bulk foam experiments. The oil was injected into the cores with a syringe pump. The set-up, described in chapter 4, was used without any changes.

#### 5.2.2 Experimental procedure

The foam quality scans in the presence of oil were performed on cores at residual oil saturation. For every experiment a new core was used. For solutions no. 3, 5, 6 and

7 a foam quality scan was performed before the experiment with oil was started. In these cases the foam was killed, as described in the experimental procedure in chapter 4, before oil was introduced into the system. The following procedure was used to reach residual oil saturation:

1. Oil was injected into the top of the core with a syringe pump. Injection continued until the pressure drop over the core was constant.
2. The core was flooded with CO<sub>2</sub>, first from top to bottom, then from bottom to top (This step was only performed for the experiments with solutions 1 and 4. The low residual oil saturation seemed not to have effect on the foam, therefore this step was skipped in later experiments).
3. 8 pv of brine was injected from the bottom up in order to partly produce the oil out of the core (This was done direct after the oil was injected into the core, the oil was not aged in the core).
4. 10 pv of surfactant solution was injected, to ensure that surfactant absorption did not influence the results.

### 5.3 Results

For the core flood experiments in the presence of oil, the foam quality scans were performed in the same way as the previous core flood experiments, with the same total superficial velocity, temperature and back pressure. Six core floods were performed with cores at residual oil saturation. The foam quality scans obtained are all shown in figure 5.1.

The maximum apparent viscosity and associated  $f_g^*$  of all the surfactant solutions is summarised together with the maximum pressure gradient over the core in table 5.1. The table contains the data for both the experiments in the absence and presence of oil. The pressure drops over the core for different foam qualities can be found in Appendix B.

The same behaviour is observed as in the core flood experiments in the absence of oil: For lower foam qualities there is little difference in apparent viscosity between the surfactant solutions. Higher foam qualities resulted in a higher spreading of the apparent viscosity.

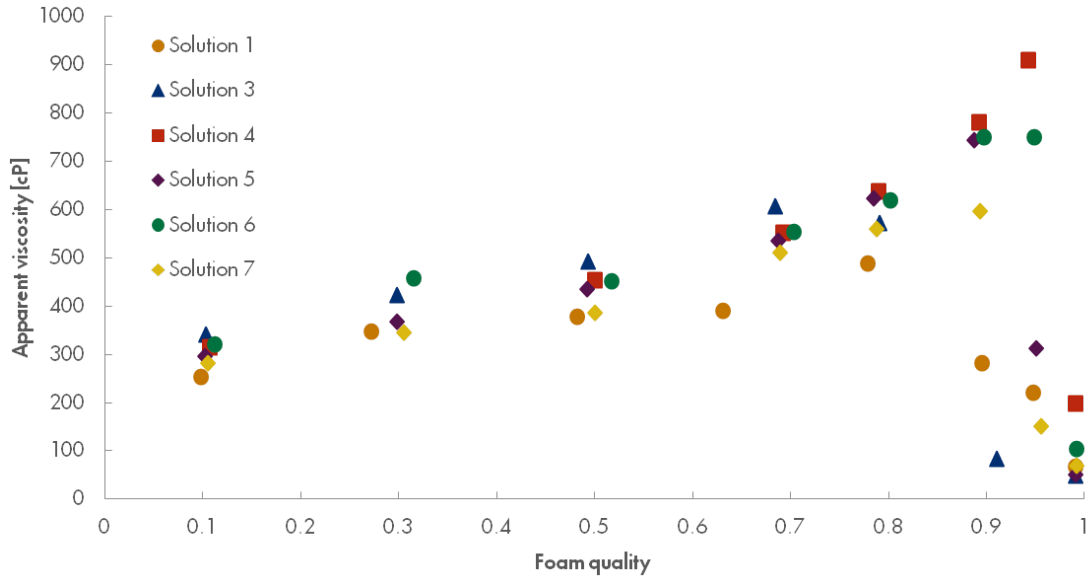


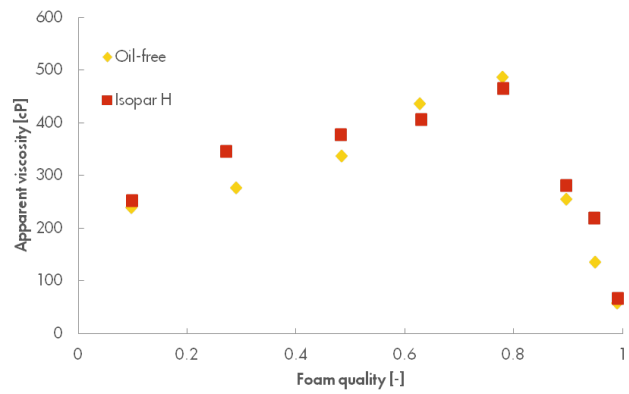
FIGURE 5.1: Foam quality scan curves for all the solutions in the presence of oil.

Solution No.	<i>In the absence of oil</i>			<i>In the presence of oil</i>		
	$\mu_{app}$ [cP]	$f_g^*$ [-]	$ \nabla P $ [Pa/m]	$\mu_{app}$ [cP]	$f_g^*$ [-]	$ \nabla P $ [Pa/m]
1	487	0.79	$52.5 \cdot 10^5$	486	0.78	$50.6 \cdot 10^5$
3	504	0.74	$57.5 \cdot 10^5$	606	0.68	$62.4 \cdot 10^5$
4	854	0.97	$89.7 \cdot 10^5$	908	0.94	$95.3 \cdot 10^5$
5	741	0.89	$79.8 \cdot 10^5$	742	0.89	$78.2 \cdot 10^5$
6	925	0.97	$96.5 \cdot 10^5$	749	0.95	$86.5 \cdot 10^5$
7	750	0.89	$74.5 \cdot 10^5$	595	0.89	$71.8 \cdot 10^5$

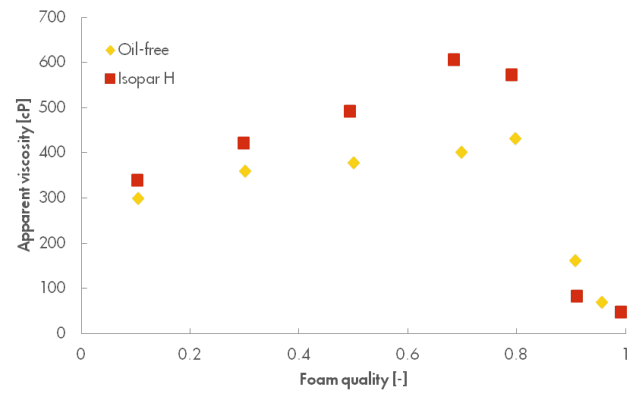
TABLE 5.1: The performance of all the surfactant solutions, both in the presence and absence of oil.

The results of the core floods in the presence and in the absence of oil are plotted together in the figure 5.2. Two types of behaviour are observed when comparing the foam quality scans:

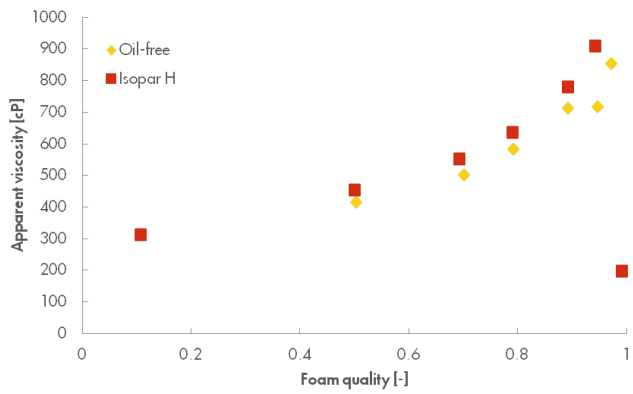
- For half of the tests, the apparent viscosity measured in the presence of oil is higher than the apparent viscosity measured in an oil free core. This occurred for the core floods performed with solution no 1,3 and 4.
- The foam quality scan curves in the absence and the presence of oil turn out to be very similar. For the low quality regime, most of the points on the foam quality scan are not influenced by the presence of oil. But around  $f_g^*$ , the oil reduced the apparent viscosity. This behaviour was observed for solution 5, 6 and 7.



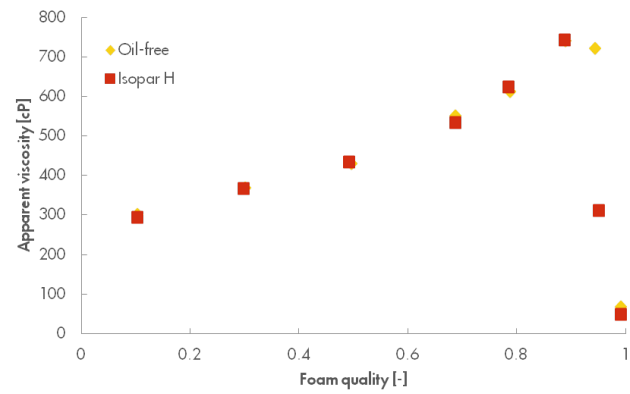
(A) Solution 1



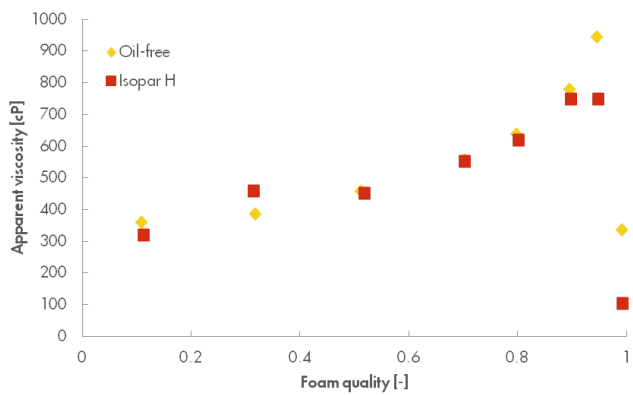
(B) Solution 3



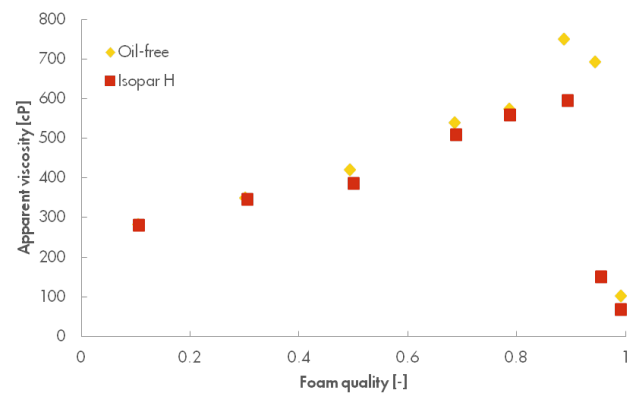
(C) Solution 4



(D) Solution 5



(E) Solution 6



(F) Solution 7

FIGURE 5.2: The performance of the different surfactant solution in porous media in the presence of oil and in an oil free porous media.



## 5.4 Discussion

### 5.4.1 Oil saturation

Due to the small pore volume of the Lilliput core and the relative big system volume, it is difficult to determine the residual oil saturation in the core. Therefore a very accurate measurement of the oil injected into the core and the oil produced out of the core is needed. The injected oil is accurately measured by the injection pump, but problems were encountered when measuring the produced oil. Some of the oil came out of the core as an emulsion. The exact volume of the emulsified oil was difficult to determine. Another problem with this set-up is the relative large volume (compared to the pv) of oil that can be trapped in the junctions of lines. This makes it difficult to determine the volume of oil remaining in the core.

The remaining oil saturation in the core is probably very low. The capillary number is defined as the ratio of the viscous forces that drive the oil out and the capillary forces that trap the oil:

$$N_{ca} = \frac{\mu_{app} \cdot u}{\phi \gamma_{OS}} \quad (5.1)$$

where  $\mu_{app}$  is the apparent viscosity,  $u$  the Darcy velocity,  $\phi$  the porosity and  $\gamma_{OS}$  the interfacial tension between the surfactant solution and oil. A higher capillary number results in a lower residual oil saturation. Figure 5.3 shows the capillary number calculated for all the solutions tested at different foam qualities.

The capillary number in a general water flood is around  $10^{-6}$ , capillary numbers of  $10^{-2}$  indicate residual oil saturation close to a zero<sup>49</sup>. In the current experiments, the high pressure gradient over the core resulted in a high apparent viscosity and the low interfacial tension resulted in relatively big capillary numbers. It is therefore highly likely that most of the oil is displaced during the foam flood. The results obtained are therefore probably just an indication of the performance of the surfactant solutions in the absence of oil. The data with oil practically reproduces the results without oil (table 5.1).

### 5.4.2 Discussion of experimental results

In the core floods performed with solutions 5, 6 and 7 there is no difference observed in the apparent viscosity in the low foam quality regime. However, more time is needed to reach a steady pressure drop at the start of a foam quality scan. Figure 5.4 shows two

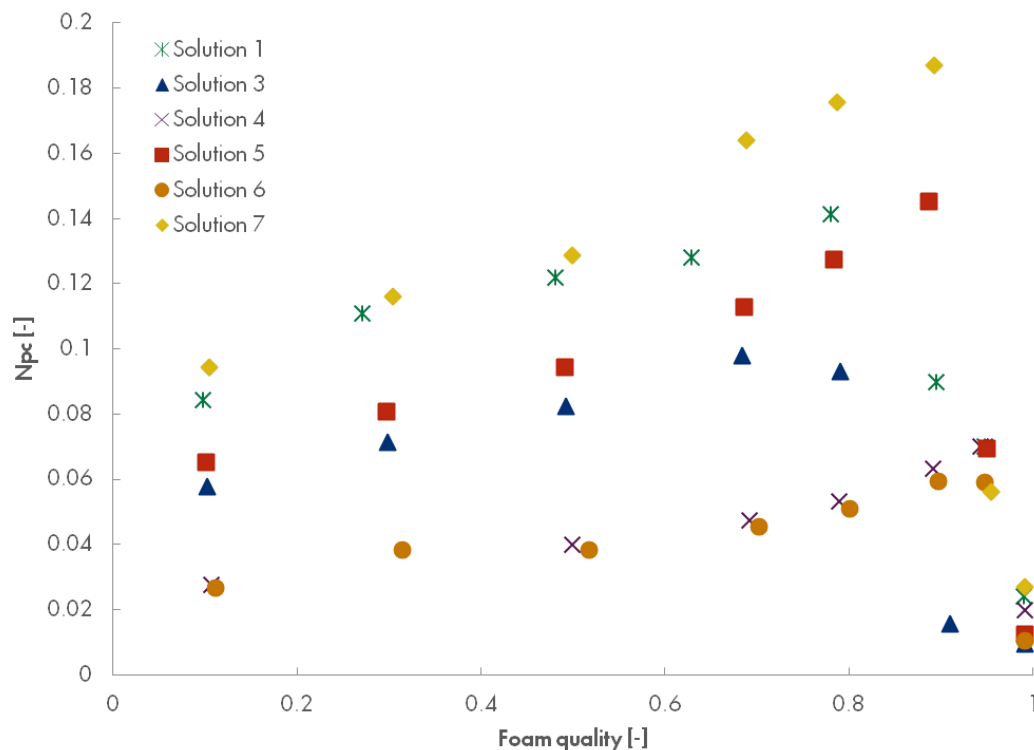


FIGURE 5.3: The capillary number at different foam qualities.

curves, one is obtained in a clean core and one in a core at residual oil saturation. For the core with oil 43 pore volumes were injected before stability was reached.

An explanation for this observation is, that the oil in the core is responsible for lamellae breakage. While the foam is generated, oil is produced out of the core. Due to the decreasing oil saturation less lamellae break and the pressure drop increases. This continues until the oil saturation is low enough not to be detrimental to foam any more.

Even though the oil is not detrimental to foam at lower foam qualities, at higher foam qualities the oil can still cause lamellae breakage. The liquid fraction is lower and the capillary pressure higher. The liquid films in the core are then more sensitive to oil. It could be that due to the high capillary pressure oil is sucked into the foam films. Another possibility is that the liquid films that are coating the wall and some of the oil filled pores become too thin to wet the oil and cause lamellae breakage.

The results of the experiments with solutions 1, 3 and 4 show that for these solutions a higher apparent viscosity is obtained with oil than without oil. Previously cases have been reported where adding oil results in a more stable foam, but this has only been observed in bulk foam experiments<sup>50,51</sup>. In such cases oil accumulate in the plateau

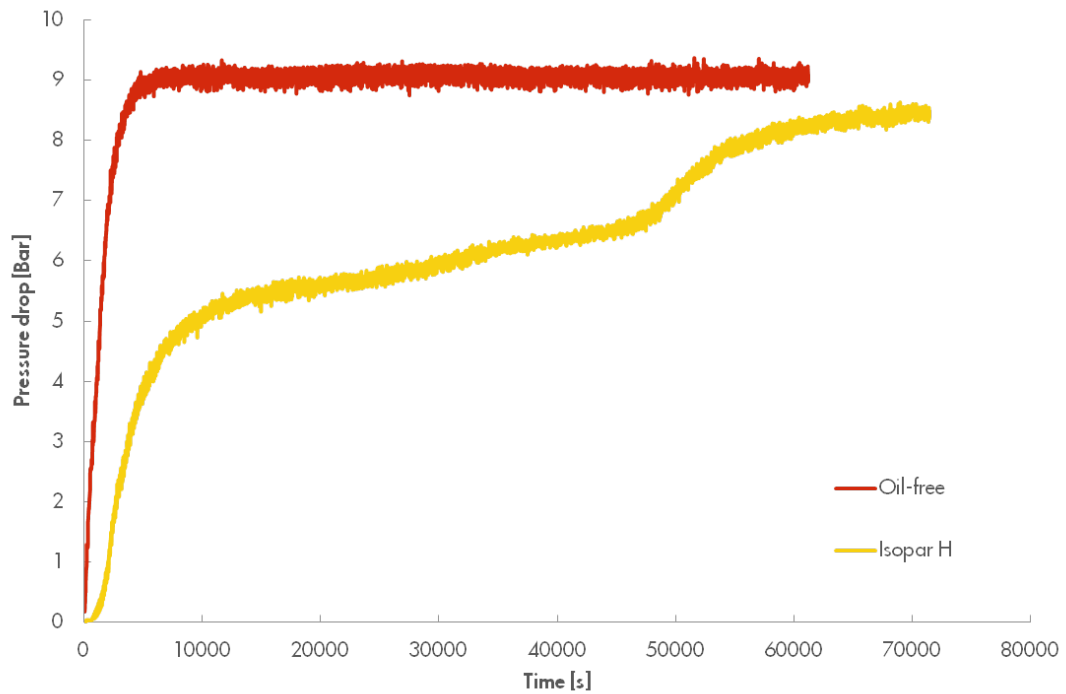


FIGURE 5.4: This graph shows the amount of time needed to reach a steady pressure drop with and without oil. The data was obtained with solution 7 at a foam quality of 0.5

borders, reducing the drainage of the foam. For the single foam films in porous media, this effect is unimportant.

For the experiments with solution 1 and 4 a  $\text{CO}_2$  flood was performed initially on the oil saturated core. It could be that in these experiments the residual oil saturation is too low to destabilise the foam at any foam quality and the difference in apparent viscosity can be attributed to experimental scatter.

There was no  $\text{CO}_2$  flood performed in the experiment with solution 3. It could be that when oil is introduced in the system it blocks off some flow paths. This would create a higher pressure drop over the core and therefore a higher apparent viscosity. The apparent viscosity is equal with the experiment in the absence of oil, when calculated with the relative permeability measured in core saturated with oil. However, the value of the capillary number suggests that all the oil is produced out of the core. There is no explanation why the apparent viscosity in the presence of oil is higher than in the absence of oil.

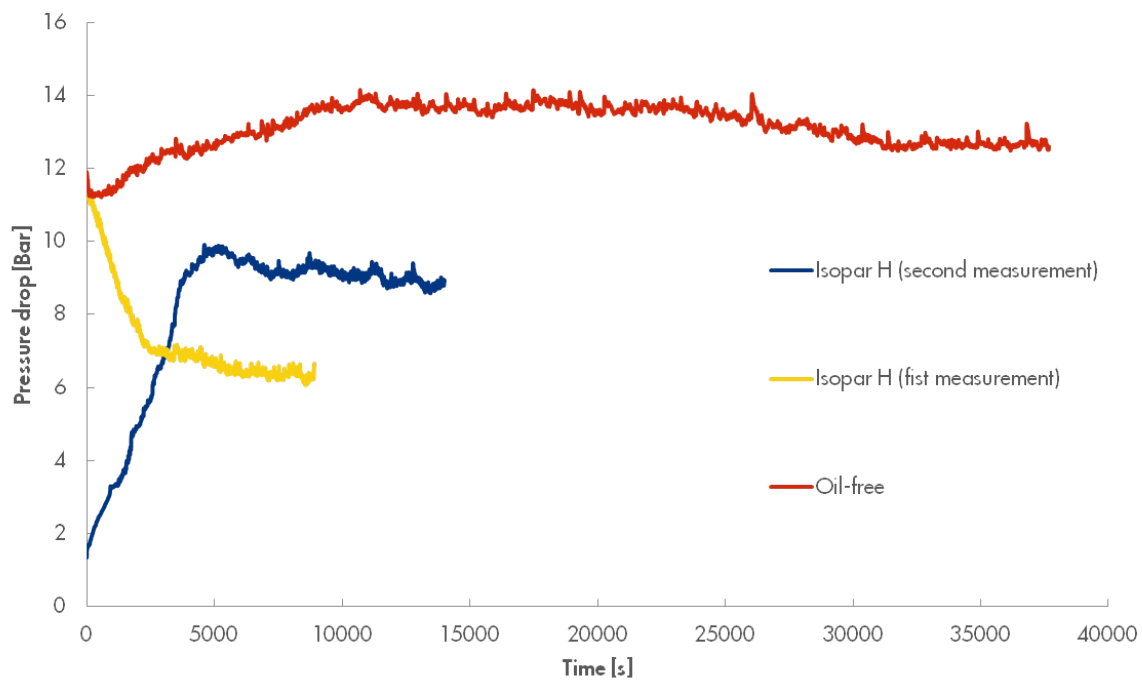


FIGURE 5.5: The measured pressure drop over time is shown. The first measurement with oil is done at the beginning of the experiment and the second measurement at the end of the experiment. The tests are performed with solution 5 at a foam quality of 0.05

### 5.4.3 Residual oil saturation during the experiment

Figure 5.5 shows two pressure curves in the presence of oil and a pressure curve in the absence of oil as a reference. The foam qualities and injection rates are equal in each case, but the pressure drops over the core differs for the first and second measurements with oil. The difference between these measurements is the stage of the experiment at which they were obtained. The first measurement was carried out at the beginning of the experiment and the second measurement at the end of the experiment, after multiple foam qualities had been tested. The reason for this difference in pressure drop is that the oil saturation in the core has been reduced. This gives a strong indication that oil is produced during the foam quality scan.

### 5.4.4 Stability criteria

For results of the core flood experiments in the presence of oil, the predicting value of the three coefficients (entering, spreading, bridging) and the lamella number is compared with the maximum apparent viscosity. Table 5.2 shows the coefficients together with

the lamella number and apparent viscosity for every used solution. The most stable foam is predicted correct by S, B and L. However, there is no correlation found between apparent viscosity and the coefficients.

There is a relation between apparent viscosity and the lamella number observed. However, the performance in the absence of oil gave the same correlation. Therefore the correlation is probably coincidence and not useful to predict the foam stability in the presence of oil.

The results of the core flood experiments are probably an indication of the performance of the surfactant solutions in the absence of oil. This makes it impossible to conclude anything about the usefulness of the coefficients and the lamella number with the performed tests.

Solution No.	E	S	B	L	$\mu_{app}^*$ [s]
1	4.47	3.85	172.49	11.03	486
3	6.97	5.75	277.92	6.15	606
4	4.04	1.68	116.19	2.73	908
5	3.83	2.89	136.77	7.02	742
6	6.53	3.99	225.37	2.82	749
7	3.83	2.49	128.24	4.88	595

TABLE 5.2: The different coefficients and the lamella number listed in one table. Green indicates the best and red the worst performance (actual or predicted)  $\mu_{app}^*$  in the presence of oil.

## 5.5 Conclusions

The apparent viscosity of foam, created using six different surfactant solutions, was determined in core flood experiments. The core floods were performed at residual oil saturation. The following conclusions were obtained:

- The high capillary numbers suggest that most of the oil is produced out of the core. Therefore it is suggested that the results show the foam behaviour in the absence of oil. The data with oil practically reproduce the results without oil.
- The saturation at which oil becomes detrimental to foam is foam quality dependent. At lower foam qualities the foam is stable in the presence of oil, while at higher foam qualities the foam is destabilised by the oil.

- 
- There is no correlation found between the entering, spreading and bridging coefficient and the lamella number. The apparent viscosities are more telling something about the performance in the absence of oil due to the probably very low oil saturation. Therefore it is not possible to conclude anything about the usefulness of the coefficients and the lamella number.
  - A big difference between core flood experiments in the presence and the absence of oil is the time needed to reach a steady pressure drop over the core during the first foam flood, oil is probably produced. When the oil saturation in the core decreases the foam stability increases. This continues until an oil saturation is reached that is not detrimental to foam and a stable pressure drop is reached.
  - Oil saturation is an important parameter when evaluating foam stability in the presence of oil. The lack of information about the residual oil saturation at different tests makes it difficult to make a comparison of the performance of the different surfactant solutions.

## Chapter 6

# Relation between bulk foam and porous media foam

### 6.1 Bulk foam and foam in porous media

One of the goals of this study is to find properties of the bulk foam that predict how the surfactant solution will perform during a core flood. There are significant differences between foams in porous media and bulk foams. In order to correlate the behaviour of bulk foams and foams in porous media it is important to understand the similarities and difference between the two types of foam.

The bulk foam created with the Foamscan device is not indefinitely stable, and does eventually collapse. The mechanisms responsible for the foam decay are gravity drainage coalescence and coarsening. The average bubble size increases because of two effects; coarsening, the diffusion of gas from the smaller bubbles to the bigger ones and coalescence, the rupture of thin films that separate adjacent bubbles.

The structure of foam in porous media differs from the polyhedral foam structure encountered in dry bulk foam. In porous media, the gas is dispersed within a continuous liquid phase with gas flow paths, in which lamellae separate the gas phase.

In porous media gravity drainage is not important for the small films in the core. On the short length scales, the hydro static pressure differences due to gravity are small and the capillary forces dominate. The two mechanisms that cause foam coalescence in porous media are capillary-suction and gas diffusion<sup>40</sup>. Capillary suction is the main cause of lamellae rupture<sup>52</sup>.

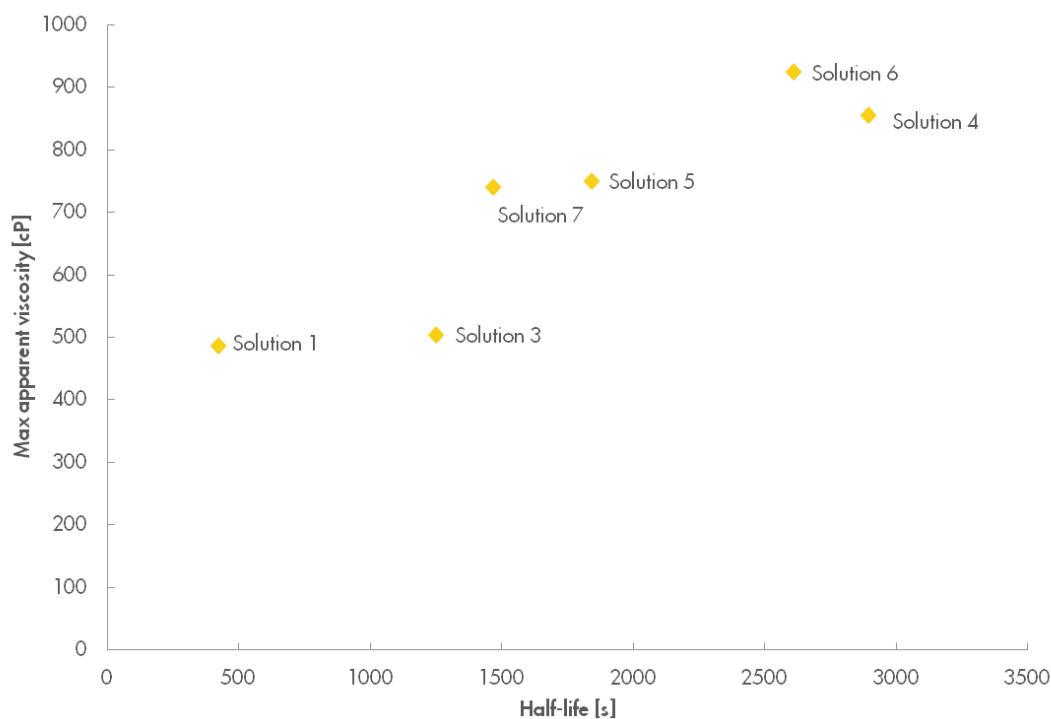


FIGURE 6.1: The half-life and maximal apparent viscosity of the used surfactant solutions plotted in one graph.

Another difference between bulk foam and foam in porous media is that the stability of the bulk foam was measured after the foam was generated, whereas the measurements in the core were performed while there was a constant generation of foam films.

Despite the many structural differences between the two foams plotting the apparent viscosity in the core as a function of the half-life of the bulk foam shows a clear relation between the two (figure 6.1). Surfactant solutions that generate more stable bulk foam create a foam with a higher apparent viscosity in porous media.

It is remarkable that the foams which are at first sight very different, correlate well. The following explanation is proposed for this correlation between foam performance in core floods and bulk foam stability.

Khristov et al.<sup>53</sup> found that bulk foam has a stability that depends on a limiting capillary pressure. Bulk foam on the other hand breaks at much lower capillary pressures than single films. Khristov et al.<sup>53</sup> attributed this to the films in the bulk foams, that have larger radii than the single films, and the "collective effects," where disturbances from the rupture of one film cause its neighbours to break as well. Bulk foam stability and the maximal apparent viscosity of foam in porous media are both related to the capillary pressure, which a single foam film can withstand.



Solution No.	$\mu_{bulk}$ (55.0 °C) [mPa·s]	Average bubble radius [mm]
1	0.5976	0.170
3	0.5788	0.191
4	0.5428	0.174
5	0.6640	0.199
6	0.6664	0.184
7	0.5545	0.202

TABLE 6.1: The viscosities of the bulk liquid, measured at 55.0 °C

There are difficulties when considering the limiting capillary pressure in bulk foam, as it occurs at a critical liquid fraction, and is therefore gravity drainage related<sup>11</sup>. Consequently, bulk foam stability can only give a proper indication about performance in the core, when the parameters, that influence the drainage rate are similar. The difference in bubble size (smaller bubbles drain slower) and viscosity should therefore be reasonable small. For all the solutions the foam was generated with the Foamscan apparatus at an equal gas flow rate, therefore the difference in bubble size was relatively small (table 6.1). The measured viscosities of the used solutions (table 6.1) do not deviate much from each other.

## 6.2 Bulk foam and foam in porous media in the presence of oil

The measured maximum apparent viscosity and the half-life in the presence of oil do not correlate (figure 6.2). However, it should be noted that for the experiments with oil, the oil is produced out of the core before the maximum apparent viscosity was reached. The performance of the surfactant solutions matched well with bulk foam experiments in the absence of oil.

## 6.3 Conclusions

In the absence of oil, bulk foam stability gives a good indication on how the surfactant will perform in a core flood, but it is probably only useful to compare solutions with a relative small difference in viscosity between the bulk fluids and foams with equal bubble sizes. The results of the core flood experiments in the presence of oil did not give a good indication of the performance of the different types of surfactants in the presence of oil.

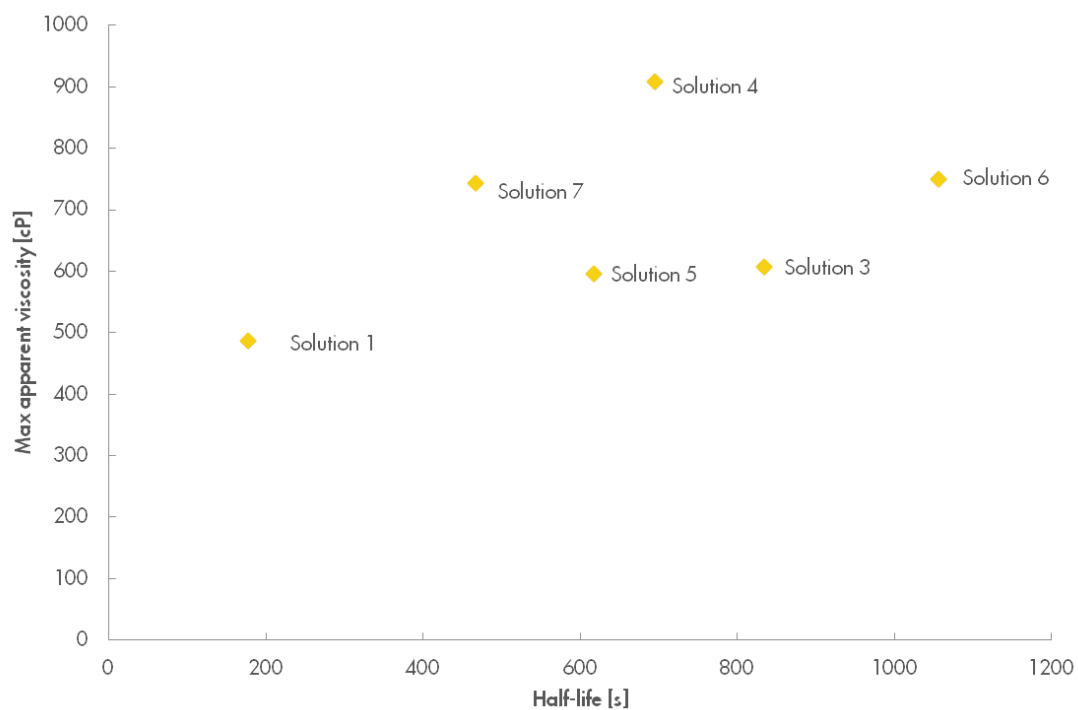


FIGURE 6.2: The half-life and the maximal apparent viscosity of the surfactant solution in the presence of oil.

It is therefore impossible to conclude if bulk foam experiments in the presence of oil are useful as a screening method.

# Chapter 7

## Curve fitting

### 7.1 Introduction

The data obtained with the core flood experiments in the absence of oil can be used to find the input parameters for a widely used foam model, the commercial reservoir simulator STARS. The parameters are determined by fitting a model curve to the experimental data. The main objective of this chapter is to examine which parameters are influenced by the surfactant type.

### 7.2 STARS model

The STARS model assumes that the apparent viscosity of the foam is a function of the relative permeability of the wetting and the non-wetting phase. The relative permeability of the water,  $k_{rw}$ , is unaffected by the foam and is only a function of the water saturation. The apparent viscosity of the foam can be defined as:

$$\mu_{app} = \frac{1}{k_{rg}^f/\mu_g + k_{rw}/\mu_{water}} \quad (7.1)$$

where  $k_{rg}^f$  is the gas relative permeability with foam,  $\mu_g$  is the viscosity of the gas phase,  $\mu_{water}$  is the viscosity of the liquid phase. The gas relative permeability in the presence of foam is given by:

$$k_{rg}^f = k_{rg} \cdot FM \quad (7.2)$$

where  $FM$  is a multiplying factor, smaller than one, that describes the reduction in gas relative permeability by the foam. In the current used model  $FM$  is a function of two other quantities  $F2$  and  $F5$ .

$$FM = \frac{1}{1 + fmmob \cdot F2 \cdot F5} \quad (7.3)$$

where  $fmmob$  is the gas mobility reduction factor for wet foam.  $F2$  represents the effect of water saturation and  $F5$  represents the shear thinning effects.

$$F2 = 0.5 \cdot \frac{\arctan(epdry \cdot (S_w \cdot fmdry))}{\pi} \quad (7.4)$$

$F2$  depends on two parameters,  $epdry$  controls the abruptness of the foam collapse as a function of the water saturation.  $fmdry$  is equal to  $S_w^*$  if the transition between the low quality and the high quality regime is abrupt<sup>54</sup>.  $F2$  is defined as:

$$F5 = \left( \frac{fmcap}{N_{ca}} \right)^{epcap} \quad (7.5)$$

where  $fmcap$  is equal to the smallest capillary number encountered and  $epcap$  describes the shear thinning behaviour. The capillary number  $N_{ca}$  is defined as:

$$N_{ca} = \frac{\mu_{app} \cdot u}{\gamma_{GS}} \quad (7.6)$$

where  $u$  the total flow rate through the pores, and  $\gamma_{GS}$  the surface tension of the surfactant solution.

The reduction of the gas relative permeability,  $FM$ , consists in this case of five parameters:  $fmmob$ ,  $epdry$ ,  $fmdry$ ,  $fmcap$  and  $epcap$ .

### 7.3 Results and discussion

The parameters are determined such that the model curves had the best match in the transition from the low to the high quality regime. The model curve is fitted to the experimental data of the core floods in the absence of oil, an example of a fit is shown in figure 7.1. The other curves can be found in Appendix C.

In the low foam quality regime, the experimental data and the curves are very different. The model curves show a shear thinning behaviour, expected due to the bubble

Solution No.	$fmmob$	$epdry$	$fmdry$	$fmcap$	$epcap$
1	2.70E+04	1.40E+02	0.32	2.06E-05	0.002
3	2.10E+04	1.20E+02	0.31	2.06E-05	0.002
4	3.60E+04	3.00E+02	0.22	2.06E-05	0.002
5	3.50E+04	1.00E+02	0.25	2.06E-05	0.002
6	4.10E+04	3.00E+02	0.25	2.06E-05	0.002
7	3.40E+04	2.50E+02	0.28	2.06E-05	0.002

TABLE 7.1: Overview of values of the five parameters from the STARS model used to fit the data.

trapping and releasing mechanism. The results of the Lilliput core flood experiments deviate significantly and show a shear thickening behaviour in the low quality regime. As described in chapter 4, the observed shear thickening can be a result of the pressure measurement over the whole core. The parameters that gave the best fit are shown in table 7.1.

For all the solutions,  $fmcap$  and  $epcap$  are equal, although the shear thickening behaviour of the experimental results make it impossible to accurately match the curve in the low quality regime of the experimental data. It was found that  $fmmob$  is the parameter that is most influenced by the surfactant performance.  $fmdry$  is also related to the surfactant type, a higher disjoining pressure will probably result in foam that will be stable at a lower water saturation.  $fmdry$  and  $epdry$  are related to each other; if the saturation at which the high quality regime is entered is higher, then the collapse must be more abrupt.

## 7.4 Conclusions

The following conclusions can be drawn from the curve fitting:

- In the low quality regime the experimental data and the model do not match well, as the shear thinning behaviour in the model is not observed in the experimental data.
- $fmmob$  is related to the surfactant type. This parameter correspond to the maximum attainable mobility reduction and is therefore most influenced by the performance of a surfactant solution.
- $fmdry$  is also related to surfactant type; higher disjoining pressure will probably result in foam that will be stable at a lower water saturation and higher capillary pressure.

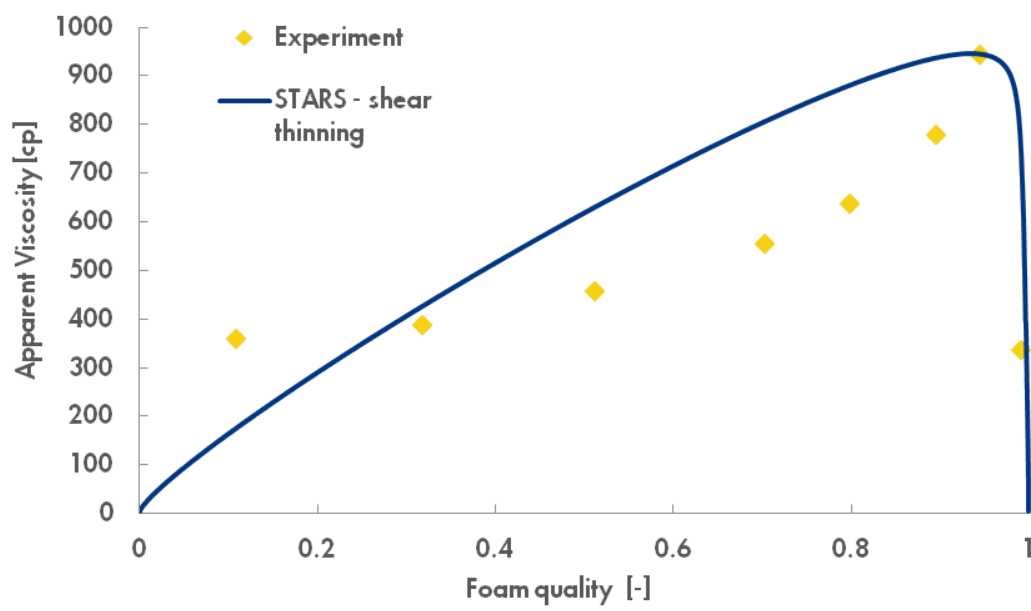


FIGURE 7.1: An example of the modelled curve and the experimental data.

## Chapter 8

# Conclusion and future directions

### 8.1 Conclusion

Foam performance has been evaluated for seven commercial surfactants using several experimental methods. Firstly, bulk foam experiments both in the presence and absence of oil were carried out. The effect of oil on the foamability and foam stability was studied. The stability criteria that predict foam stability in the presence of oil were analysed. Secondly, core flood experiments in absence of oil were carried out. The performance of different surfactant solutions was examined. Thirdly, core floods were performed on cores at residual oil saturation. The effect of oil on foam stability was studied. A summary of the main findings obtained from this thesis is given below.

- In the absence of oil, there is a correlation between bulk foam stability and core flood performance. More stable bulk foam results in a higher apparent viscosity in core flood tests. Therefore, bulk foam experiments could be a useful screening tool providing a good indication of the surfactants performance in the core.

In the presence of oil, no correlation was found between bulk foam stability and the performance in the core. The results of the bulk foam experiments in the presence of oil do not give a good indication of the performance of different types of surfactants in the presence of oil. It is therefore impossible to conclude if bulk foam experiments in the presence of oil are useful as a screening method.

- Introducing oil reduced the bulk foam stability for all the surfactant solutions tested. The extent of stability reduction was related to surfactant type. For the bulk foam experiments in the presence of oil, a relation between the interfacial tension and the foam half-life was observed. The lower the interfacial tension between the oil and the surfactant solution, the shorter the foam half-life. The

entering, spreading and bridging coefficients and the lamella number did not give reliable predictions for the stability of a bulk foam in the presence of oil.

- In the core flood experiments in the absence of oil, all the surfactant solutions had an equal apparent viscosity for foam qualities up to 0.70. At higher foam qualities, differences in performance were observed between the solutions. The apparent viscosity can be affected by the Gibbs-Marangoni effect, but more experiments are needed to study this effect. It is suggested that the best performing solutions were the solutions that endure the capillary forces the best. There is a clear relation between  $f_g^*$  and the maximum apparent viscosity; a higher  $f_g^*$  results in a higher maximum apparent viscosity.
  - The low interfacial tension of the surfactant solution with the oil and the high apparent viscosity of the foam in the core resulted in high capillary numbers. This suggests that most of the oil was produced out of the core during the tests. Therefore, it is likely that the results obtained are showing the foam behaviour without oil. The data with oil almost exactly reproduce the results without oil. The observed effect of the oil was the increase in time needed to reach a steady pressure drop over the core during the first foam flood. As a result, oil was produced during this extra time as the test was running. The oil saturation in the core decreases and the foam stability increases. This continues until an oil saturation is reached that is low enough to be not detrimental to foam any more and a stable pressure drop is reached. The saturation at which oil becomes detrimental to foam is foam quality dependent. At lower foam qualities the foam is always stable in the presence of oil, while at higher foam qualities the foam is destabilised by the oil.
  - In the core flood experiments in the presence of oil the entering, spreading and bridging coefficient and the lamella number were not able to predict the behaviour of the foam. Because of the very low oil saturation in the core, the measured apparent viscosities are an indication of the foam behaviour in the absence of oil. Therefore, it is not possible to conclude anything about the usefulness of the coefficients and the lamella number in porous media.
  - In the low quality regime, the experimental data and the model curve did not match, the shear thinning behaviour in the model is not observed in the experimental data. The gas mobility reduction factor for wet foam,  $f_{mmob}$ , is surfactant type related. This parameter is most influenced by the performance of a surfactant solution.
-



## 8.2 Future directions

From this study was observed that the E, S and B coefficients and the lamellae number do not give accurate predictions of the stability of bulk foams in contact with oil.

It is suggested that the stability of the pseudo-emulsion film could be a better predictor for foam behaviour in the presence of oil. According to several authors (table 2.1), a stable foam in the presence of oil is related to the stability of the pseudo-emulsion film. It would therefore be useful to incorporate an investigation into pseudo-emulsion film stability in future research.

The apparent viscosity of foam in porous media is assumed to be linked to the surface elasticity of the surfactant-gas surface, although the link between the surface rheology and foam flood behaviour in porous media is not completely understood. Further research on the effect of surface-tension gradients on foam in porous media is needed.

It is suggested that the disjoining pressure is an important parameter for to the stability of individual foam films and thus the performance of surfactant solutions in a core. However, an evaluation of the disjoining pressure isotherms of the surfactants solutions used would be necessary to confirm the role of disjoining pressure in foam stability. Unfortunately, as screening tool disjoining pressure might not be very useful, because the measurements are difficult to perform. This information can be invaluable for the surfactant design. Also for the general understanding of foam in porous media, information about the disjoining pressure can give valuable insights.

## 8.3 Recommendations to improve experiment results

In order to improve the experimental test, the following recommendations have to be considered.

### 8.3.1 Recommendations for bulk foam experiments

- The experiments with oil should be repeated with a different type of oil, which also generates negative coefficients (sunflower oil is believed to have this properties). In this way the predicting value of the different coefficients can be better examined.
- It is suggested that a lower gas flow rate during the foaming stage has two benefits. Firstly a lower flow rate would give a better insight on the foamability. Secondly, less oil will be carried up during foam generation at a lower flow rate and it can be investigated if there is still a link between interfacial tension and foam stability in

the presence of oil. Measuring the quantity of oil carried up with the foam would be even more useful.

### **8.3.2 Recommendations for the core flood experiments in the absence of oil**

- It is suggested that the core flood experiments should be carried out multiple times to test the reproducibility of the experiments in used set-up.
- The pressure drop over the whole core was measured during this series of experiments. More pressure taps in the core could give better insight on the foam behaviour in the core and would provide information on the foam generating zone and the capillary end effect.
- A comparison between experimental results obtained from different core geometries could be useful to get a better understanding on the effect of core geometry. This can also determine the accuracy of the Lilliput core as a screening tool.

### **8.3.3 Recommendations for the core flood experiments in the presence of oil**

- Experiments in the presence of oil in a Lilliput core are difficult to perform, as the volume of the residual oil is small. If any oil is produced, the volume is too small and it can not be observed visually. Different techniques should be considered in order to obtain accurate information about the oil production and saturation. For example, by measuring the oil content of the effluent.
- A foam quality scan is not an optimal experimental method to evaluate the performance of surfactant solutions in the presence of oil. A better method to compare surfactant performance would be a core flood with fixed foam quality.
- During the experiments almost all of the oil was produced out of the core. A more viscous oil or a oil with a higher interfacial tension, with the surfactant solution, could prevent that all the oil is produced out of the core.

## Appendix A

# Results core flood experiments

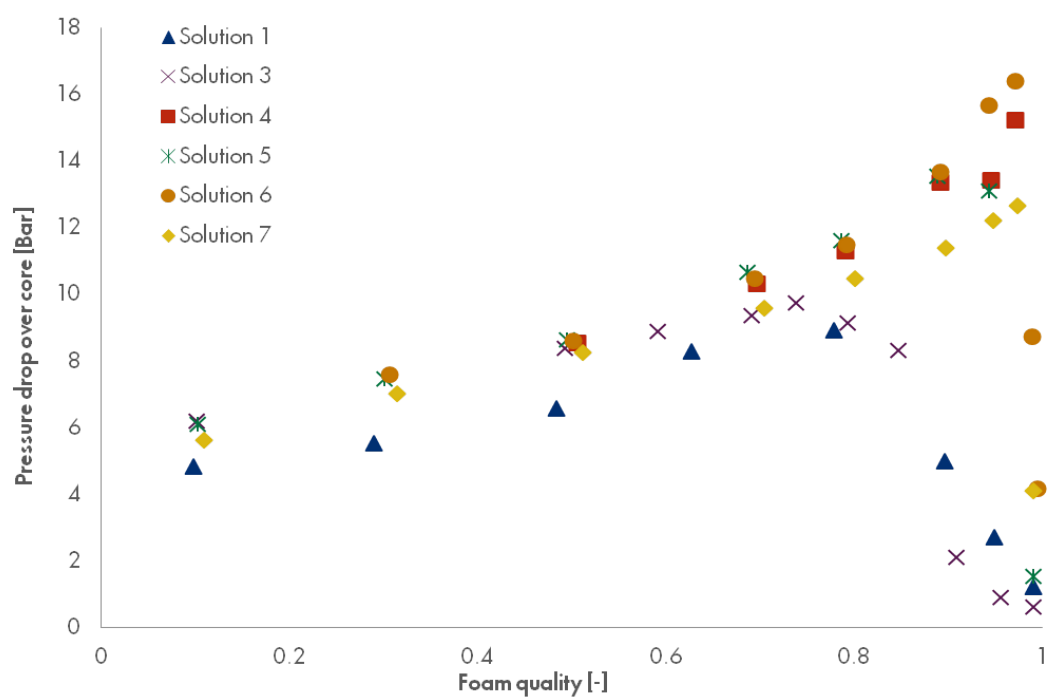


FIGURE A.1: The pressure drop over the core for all the surfactants solution measured in the absence of oil.

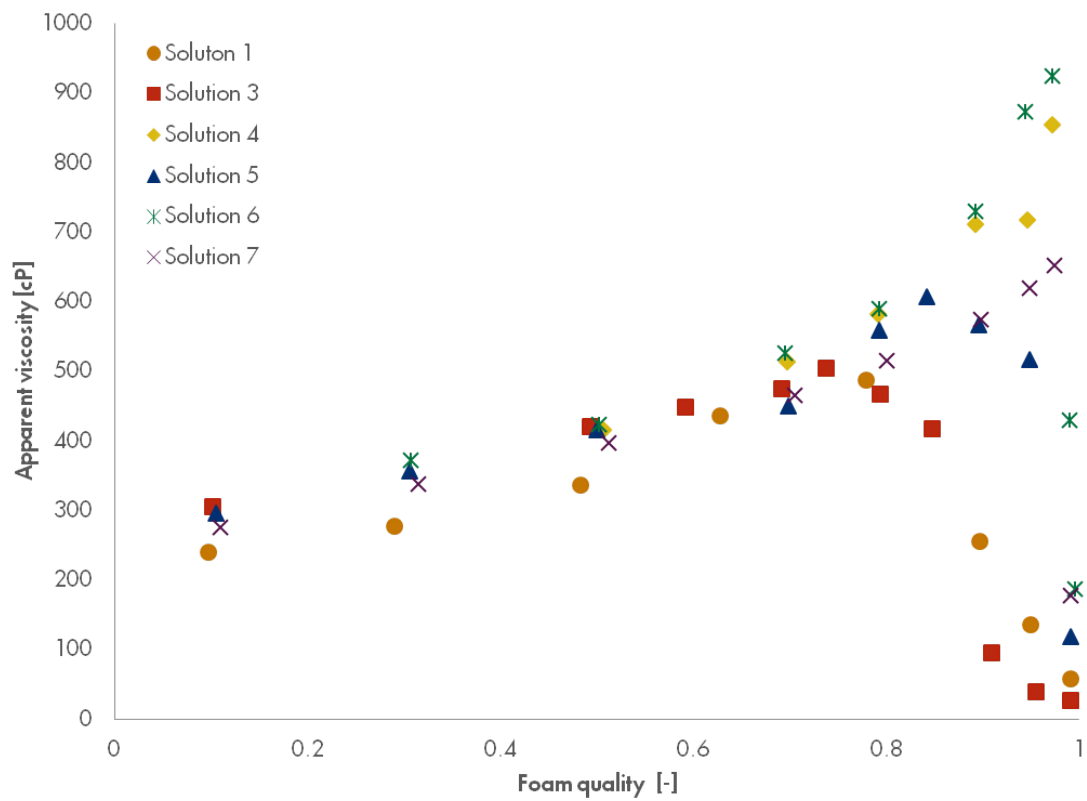


FIGURE A.2: The apparent viscosity of all the surfactant solutions at different foam qualities in the absence of oil.

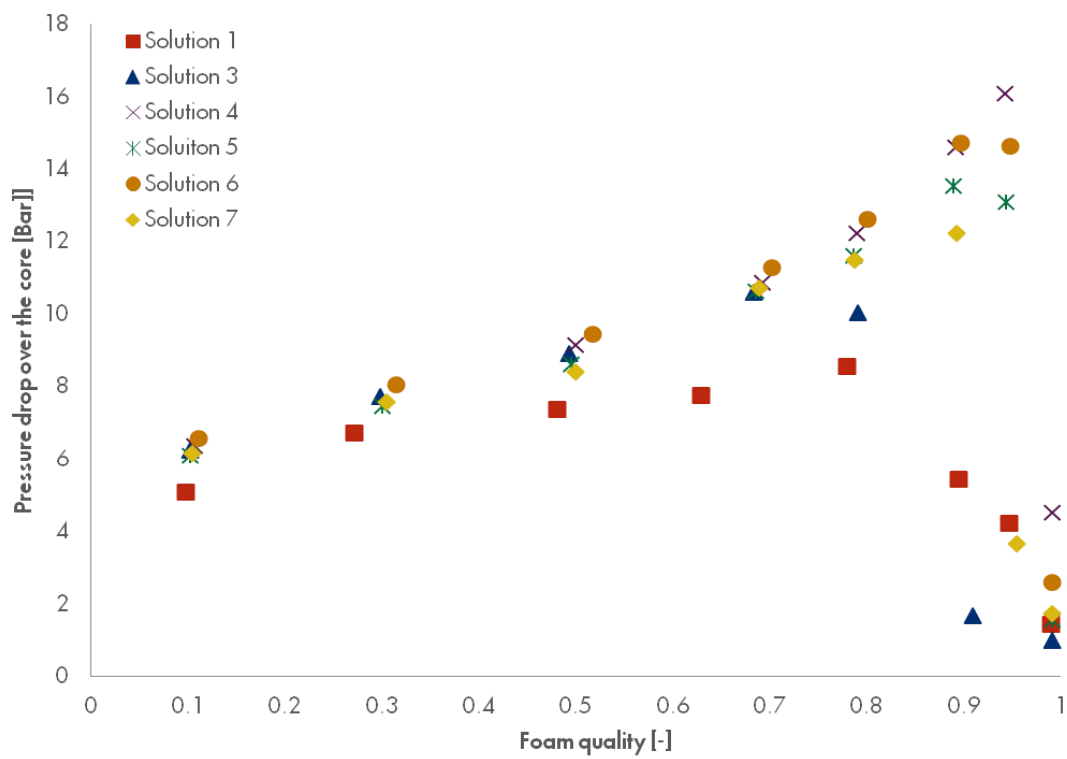


FIGURE A.3: The pressure drop over the core for all surfactant solutions measured in the presence of oil.

## Appendix B

# Interfacial rheology measurement

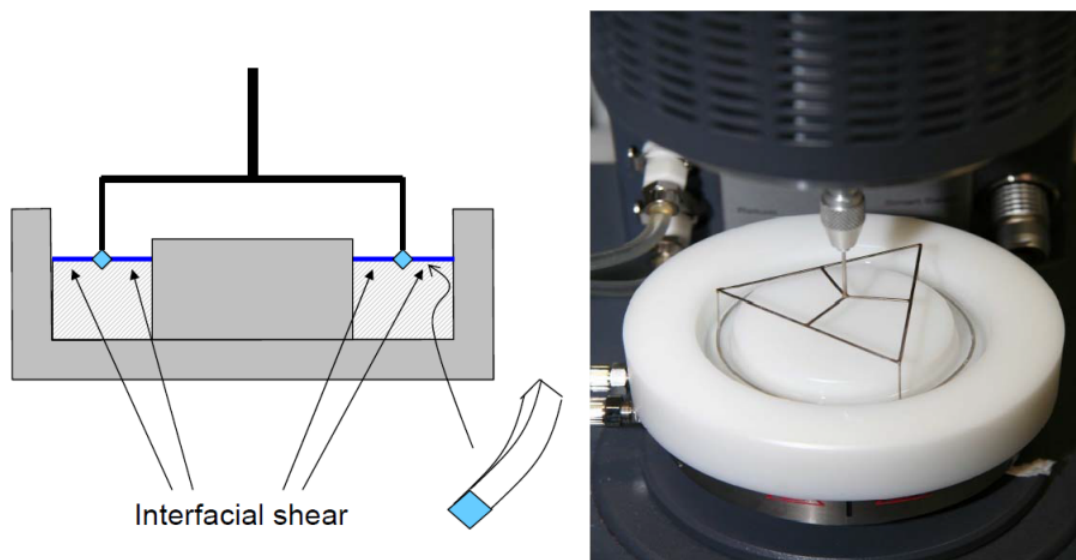


FIGURE B.1: Overview of the double wall ring rheometer. The torque is increased due to the double wall geometry of the ring used<sup>3</sup>.

## B.1 Surface rheology

Interfacial rheology provides information on the adsorption behaviour and the interaction of the surfactant molecules at the interfaces. The adsorption phenomena is important for film generation (foaming) and the stability of films<sup>3</sup>. The viscoelastic response of an interface is separated into an elastic (storage modulus) part and a viscous (loss modulus) part.

## B.2 Materials

The surface viscosity measurements for the six surfactant solutions have been conducted using a commercial surface rheometer (figure B.1). The rheometer has a double wall-ring geometry to measure the viscoelastic properties of interfaces in shear flows. The geometry of the rheometer used is shown in figure B.1. The sensitivity of this geometry has been demonstrated using reference Newtonian and viscoelastic fluids<sup>55</sup>. The current measurements were conducted at 55.0°C, the same condition as for the bulk and core flood experiments.



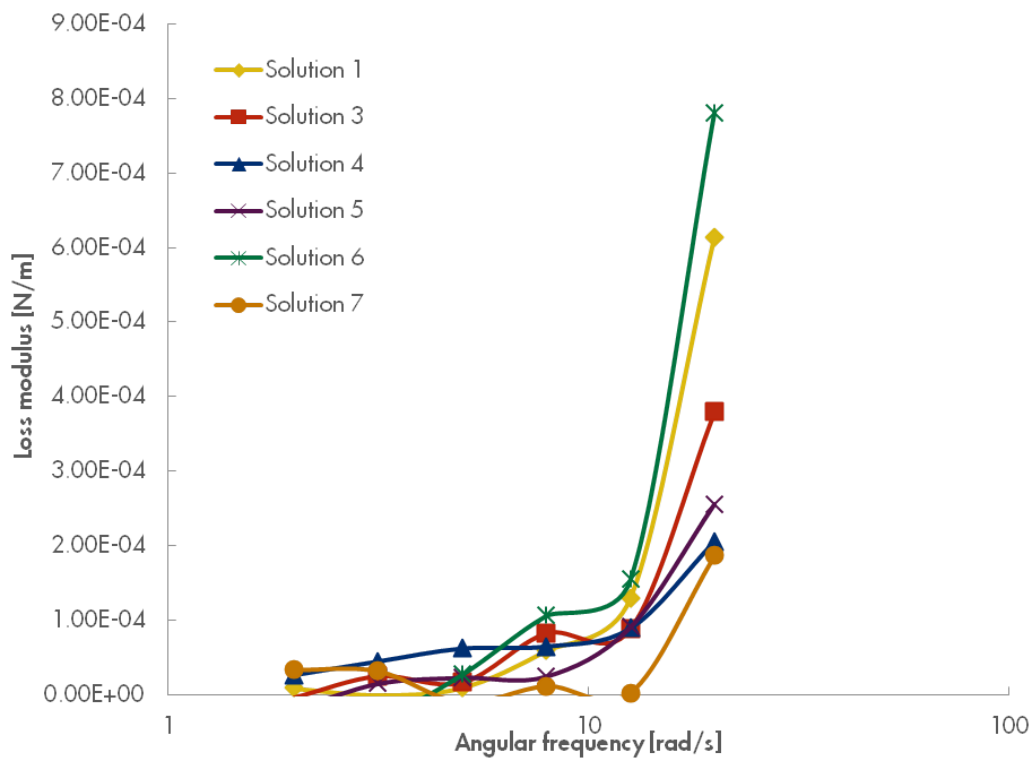


FIGURE B.2: The loss modulus as function of angular frequency for the used solutions.

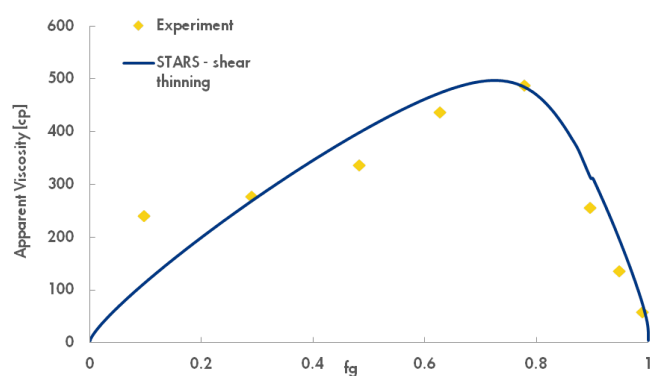
### B.3 Results

The elastic response in oscillation mode is similar for all the surfactants. The value of the elastic response is similar to the surface elasticity of water. The viscous response is different for every surfactant solution. It has been demonstrated that surface viscosity plays a key role in the film stability<sup>56</sup>. Solution 6 has the highest elasticity while solution 7 the lowest (figure B.2). There is a big difference in apparent viscosity between these two solutions in the low quality regime. This could be due to the more stable films<sup>3</sup>, Another possibility is that the films with a higher loss modulus create more drag in constrictions resulting in a higher apparent viscosity.

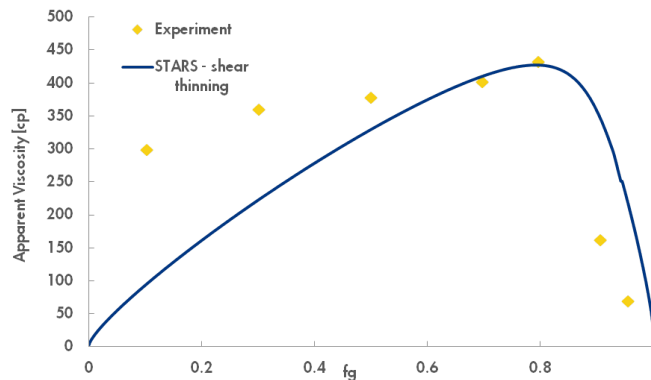


## Appendix C

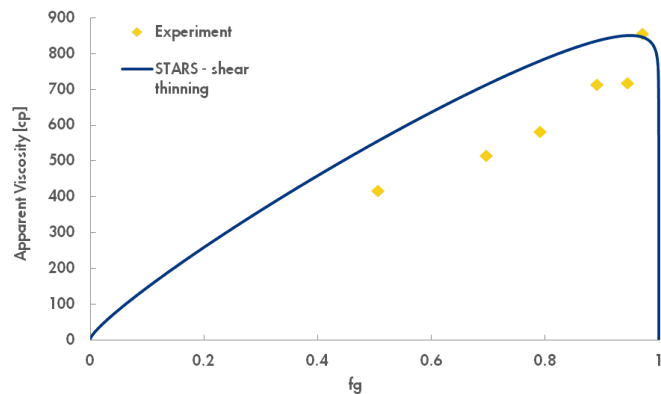
### Results curve fitting



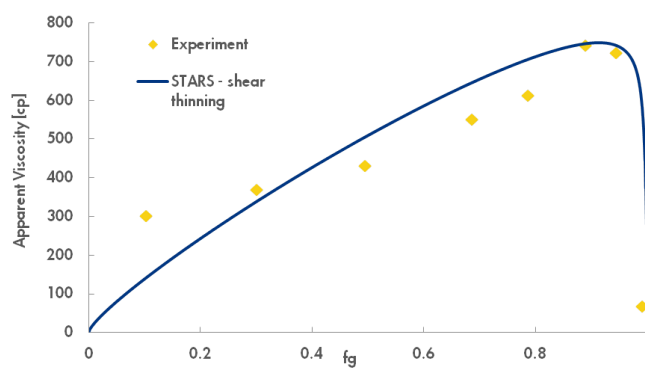
(A) Solution 1



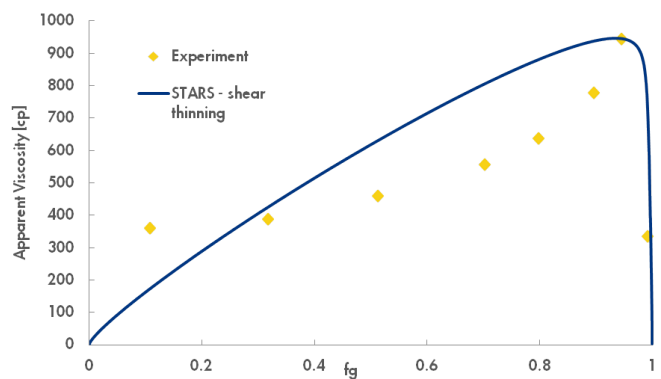
(B) Solution 3



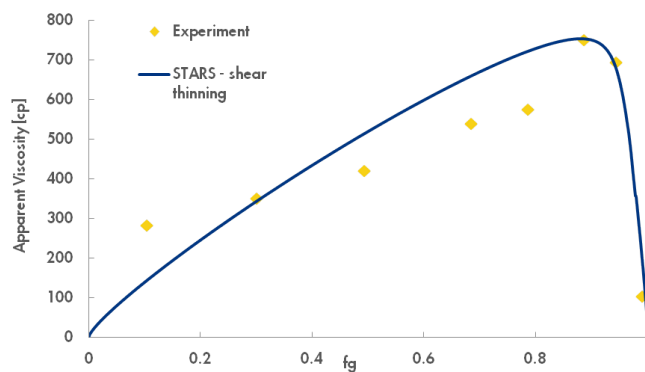
(C) Solution 4



(D) Solution 5



(E) Solution 6



(F) Solution 7

FIGURE C.1: The experimental data for the six different surfactant solutions in the absence of oil and their associated model curves.

# Bibliography

- [1] L.L. Schramm. *Foams: fundamentals and applications in the petroleum industry*. Advances in chemistry series. American Chemical Society, 1994. ISBN 9780841227194.
- [2] Konstantin G. Kornev, Alexander V. Neimark, and Aleksey N. Rozhkov. Foam in porous media: thermodynamic and hydrodynamic peculiarities. *Advances in Colloid and Interface Science*, 82(1–3):127 – 187, 1999. ISSN 0001-8686.
- [3] Gary Pope. Presentation chemical eor research program annual workshop, 2012.
- [4] F.M. Orr. *Theory of gas injection processes*. Tie-Line Publications, 2007.
- [5] L.W. Lake. *Fundamentals of Enhanced Oil Recovery*. SPE continuing education. SPE, 1986.
- [6] E.J. Koval. A method for predicting the performance of unstable miscible displacement in heterogeneous media. *Society of Petroleum Engineers Journal*, 1963.
- [7] K. Mannhardt, J.J. Novosad, and L.L. Schramm. Foam/oil interactions at reservoir conditions. *SPE/DOE Improved Oil Recovery Symposium, 19-22 April, Tulsa, Oklahoma*, 1998. ISSN 978-1-55563-387-5.
- [8] R. Farajzadeh, A. Andrianov, R. Krastev, G.J. Hirasaki, and W.R. Rossen. Foam–oil interaction in porous media: Implications for foam assisted enhanced oil recovery. *Advances in Colloid and Interface Science*, 183–184(0):1 – 13, 2012. ISSN 0001-8686.
- [9] F.E. Suffridge, K.T. Raterman, and G.C. Russell. Foam performance under reservoir conditions. *SPE Annual Technical Conference and Exhibition, 8-11 October, San Antonio, Texas*, 1989. ISSN 978-1-55563-559-6.
- [10] A.D. Nikolov, D.T. Wasan, D.W. Huang, and D.A. Edwards. The effect of oil on foam stability: Mechanisms and implications for oil displacement by foam in porous media. 1986. ISSN 978-1-55563-607-4.

- 
- [11] Olivier Pitois. *Foam Engineering: Fundamentals and Applications*, chapter Foam Ripening, pages 59–73. John Wiley & Sons, Ltd, 2012. ISBN 9781119954620.
- [12] I. Cantat, S. Cohen-Addad, F. Elias, F. Graner, R. Höhler, O. Pitois, and R. Flatman. *Foams: Structure and Dynamics*. OUP Oxford, 2013. ISBN 9780199662890. URL <http://books.google.nl/books?id=Ndzz11hUNRoC>.
- [13] J.A.F. Plateau. Statique experimentale et theorique des liquides soumis aux seules forces moleculaires. *Gauthier-Villars*, 1873.
- [14] Josiah Willard Gibbs. On the equilibrium of heterogeneous substances. part ii. *Transactions of the Connecticut Academy of Arts and Sciences*, 3:343–524, 1878.
- [15] Rossen Sedev and Dotchi Exerowa. {DLVO} and non-dlvo surface forces in foam films from amphiphilic block copolymers. *Advances in Colloid and Interface Science*, 83(1–3):111 – 136, 1999. ISSN 0001-8686.
- [16] Arnaud Saint-Jalmes. Physical chemistry in foam drainage and coarsening. *Soft Matter*, 2:836–849, 2006.
- [17] Annie Colin. *Foam Engineering: Fundamentals and Applications*, chapter Coalescence in Foams, pages 75–90. John Wiley & Sons, Ltd, 2012. ISBN 9781119954620.
- [18] Nikolai D. Denkov, Krastanka G. Marinova, and Slavka S. Tcholakova. Mechanistic understanding of the modes of action of foam control agents. *Advances in Colloid and Interface Science*, 2013. ISSN 0001-8686.
- [19] H.C. Lau and S.M. O'Brien. Effects of spreading and nonspreading oils on foam propagation through porous media. *SPE Journal Paper*, 1988.
- [20] T.S. Kristiansen and Torleif Holt. Properties of flowing foam in porous media containing oil. *Conference Paper*, 1992. ISSN 978-1-55563-507-7.
- [21] Mariann Dalland, Jan Erik Hanssen, and Tove Strøm Kristiansen. Oil interaction with foams under static and flowing conditions in porous media. *Colloids and Surfaces A: Physicochemical and Engineering Aspects*, 82(2):129 – 140, 1994. ISSN 0927-7757.
- [22] Jongju Lee, Alex Nikolov, and Darsh Wasan. Stability of aqueous foams in the presence of oil: On the importance of dispersed vs solubilized oil. *Industrial & Engineering Chemistry Research*, 52(1):66–72, 2013.
- [23] David J. Manlowe and Clayton J. Radke. A pore-level investigation of foam/oil interactions in porous media. *SPE Reservoir Engineering*, 5:495 – 502, 1990.

- [24] Karin Mannhardt, J Novosad, and L Schramm. Comparative evaluation of foam stability to oil. *SPE Reservoir Evaluation & Engineering*, 3(1):23–34, 2000.
- [25] A. Andrianov, R. Farajzadeh, M. Mahmoodi Nick, M. Talanana, and P. L. J. Zitha. Immiscible foam for enhancing oil recovery: Bulk and porous media experiments. *Industrial & Engineering Chemistry Research*, 51(5):2214–2226, 2012.
- [26] V. Bergeron, M. E. Fagan, and C. J. Radke. Generalized entering coefficients: a criterion for foam stability against oil in porous media. *Langmuir*, 9(7):1704–1713, July 1993. ISSN 0743-7463.
- [27] Laurier L. Schramm and Jerry J. Novosad. The destabilization of foams for improved oil recovery by crude oils: Effect of the nature of the oil. *Journal of Petroleum Science and Engineering*, 7(1–2):77 – 90, 1992. ISSN 0920-4105. `jcetitleEnhanced Oil Recovery` `jcetitlej`.
- [28] Laurier L. Schramm and Jerry J. Novosad. Micro-visualization of foam interactions with a crude oil. *Colloids and Surfaces*, 46(1):21 – 43, 1990. ISSN 0166-6622.
- [29] Anne Kari Vikingstad, Arne Skauge, Harald Høiland, and Morten Aarra. Foam -oil interactions analyzed by static foam tests. *Colloids and Surfaces A: Physicochemical and Engineering Aspects*, 260(1–3):189 – 198, 2005. ISSN 0927-7757.
- [30] K Koczko, L.A Lobo, and D.T Wasan. Effect of oil on foam stability: Aqueous foams stabilized by emulsions. *Journal of Colloid and Interface Science*, 150(2):492 – 506, 1992. ISSN 0021-9797.
- [31] Jongju Lee, Alex Nikolov, and Darsh Wasan. Surfactant micelles containing solubilized oil decrease foam film thickness stability. *Journal of Colloid and Interface Science*, 415(0):18 – 25, 2014. ISSN 0021-9797.
- [32] K.T. Raterman. An investigation of oil destabilization of nitrogen foams in porous media. *SPE Annual Technical Conference and Exhibition, 8-11 October, San Antonio, Texas*, 1989. ISSN 978-1-55563-559-6.
- [33] A.R. Kovscek, C.J. Radke, University of California. Department of Chemical Engineering, Lawrence Berkeley Laboratory. Earth Sciences Division, and Bartlesville Energy Research Center United States. Department of Energy. *Fundamentals of Foam Transport in Porous Media-: Topical Report*. DOE/BC. Bartlesville Project Office, U.S. Department of Energy, 1993.
- [34] PacelliL.J. Zitha, QuocP. Nguyen, PeterK. Currie, and MartenA. Buijse. Coupling of foam drainage and viscous fingering in porous media revealed by x-ray computed tomography. *Transport in Porous Media*, 64(3):301–313, 2006. ISSN 0169-3913.

- 
- [35] A.S. Aronson, V. Bergeron, M.E. Fagan, and C.J. Radke. The influence of disjoining pressure on foam stability and flow in porous media. *Colloids and Surfaces A: Physicochemical and Engineering Aspects*, 83(2):109 – 120, 1994. ISSN 0927-7757.
- [36] Amit Chakma. Interfacial phenomena in petroleum recovery, edited by Norman R. Morrow, . *The Canadian Journal of Chemical Engineering*, 71(3):493–494, 1993. ISSN 1939-019X.
- [37] George G. Bernard and W.L. Jacobs. Effect of foam on trapped gas saturation and on permeability of porous media to water. 1965.
- [38] A. R. Koval, T. W. Patzek, and C. J. Radke. Mechanistic foam flow simulation in heterogeneous and multidimensional porous media. *Society of Petroleum Engineers Journal*, 2(4):511–526, December 1997.
- [39] T.C. Ransohoff and C.J. Radke. *Mechanisms of foam generation in glass bead packs*. Jun 1986.
- [40] K. T. Chambers and C. J. Radke. *In Interfacial Phenomena in Petroleum Recovery*. 1991.
- [41] Z.I. Khatib, G.J. Hirasaki, and A.H. Falls. Effects of capillary pressure on coalescence and phase mobilities in foams flowing through porous media. 1988.
- [42] Alexander Patist, Teri Axelberd, and Dinesh O. Shah. Effect of long chain alcohols on micellar relaxation time and foaming properties of sodium dodecyl sulfate solutions. *Journal of Colloid and Interface Science*, 208(1):259 – 265, 1998. ISSN 0021-9797.
- [43] W.R. Rossen and M.W. Wang. Modeling foams for acid diversion. *PE Journal Paper*, 1999.
- [44] J.M. Alvarez, H.J. Rivas, and W.R. Rossen. Unified model for steady-state foam behavior at high and low foam qualities. *SPE Conference Paper*, 2001.
- [45] A.H. Falls, J.J. Musters, and J. Ratulowski. The apparent viscosity of foams in homogeneous bead packs. *SPE Reservoir Engineering*, 4:155 – 164, 1989.
- [46] K. Golemanov, N. D. Denkov, S. Tcholakova, M. Vethamuthu, and A. Lips. Surfactant mixtures for control of bubble surface mobility in foam studies. *Langmuir*, 24(18):9956–9961, 2008.
- [47] Arnold S. de Vries and Krijn Wit. Rheology of gas/water foam in the quality range relevant to steam foam. 1990.



- [48] R.A. Ettinger and C.J. Radke. Influence of texture on steady foam flow in berea sandstone. pages –, 1992.
- [49] Sanjay Kumar, T.F. Yen, George V. Chilingarian, and Erle C. Donaldson. Chapter 9 alkaline flooding. In George V. Chilingarian Erle C. Donaldson and Teh Fu Yen, editors, *Enhanced Oil Recovery, II Processes and Operations*, volume 17, Part B of *Developments in Petroleum Science*, pages 219 – 254. Elsevier, 1989. doi: [http://dx.doi.org/10.1016/S0376-7361\(08\)70461-8](http://dx.doi.org/10.1016/S0376-7361(08)70461-8). URL <http://www.sciencedirect.com/science/article/pii/S0376736108704618>.
- [50] J. Goyon, F. Bertrand, O. Pitois, and G. Ovarlez. Shear induced drainage in foamy yield-stress fluids. *Phys. Rev. Lett.*, 104:128301, Mar 2010. doi: 10.1103/PhysRevLett.104.128301. URL <http://link.aps.org/doi/10.1103/PhysRevLett.104.128301>.
- [51] Keyvan Piroird and Élise Lorenceau. Capillary flow of oil in a single foam microchannel. *Phys. Rev. Lett.*, 111:234503, Dec 2013.
- [52] A.R. Kovscek and C.J. Radke. *Fundamentals of foam transport in porous media*. Oct 1993.
- [53] Khr.I. Khristov, D.R. Exerowa, and P.M. Krugljakov. Influence of the type of foam films and the type of surfactant on foam stability. *Colloid and Polymer Science*, 261(3):265–270, 1983. ISSN 0303-402X.
- [54] Christian S Boeije and William Richard Rossen. Fitting foam simulation model parameters to data. 2013.
- [55] Steven Vandebril, Aly Franck, GeraldG. Fuller, Paula Moldenaers, and Jan Vermant. A double wall-ring geometry for interfacial shear rheometry. *Rheologica Acta*, 49(2):131–144, 2010. ISSN 0035-4511. doi: 10.1007/s00397-009-0407-3. URL <http://dx.doi.org/10.1007/s00397-009-0407-3>.
- [56] Benoit Scheid, Stéphane Dorbolo, Laura R. Arriaga, and Emmanuelle Rio. Antibubble dynamics: The drainage of an air film with viscous interfaces. *Phys. Rev. Lett.*, 109:264502, Dec 2012. doi: 10.1103/PhysRevLett.109.264502. URL <http://link.aps.org/doi/10.1103/PhysRevLett.109.264502>.